ETC HE Report 2024/1

Interim air quality maps of EEA member and cooperating countries for 2023

PM, O_3, and NO_2 spatial estimates

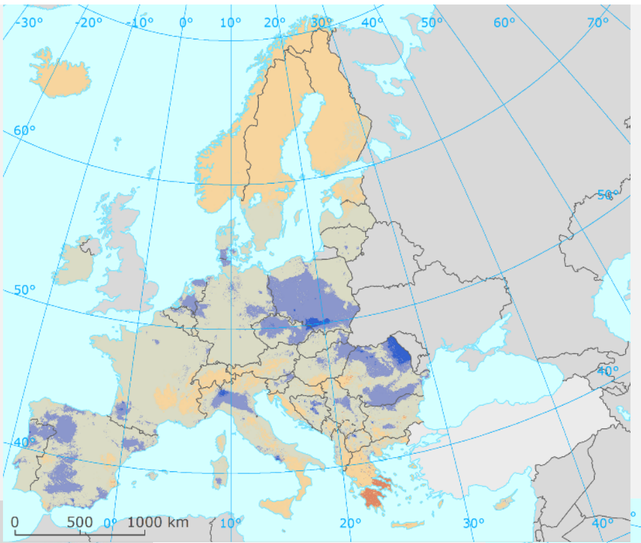

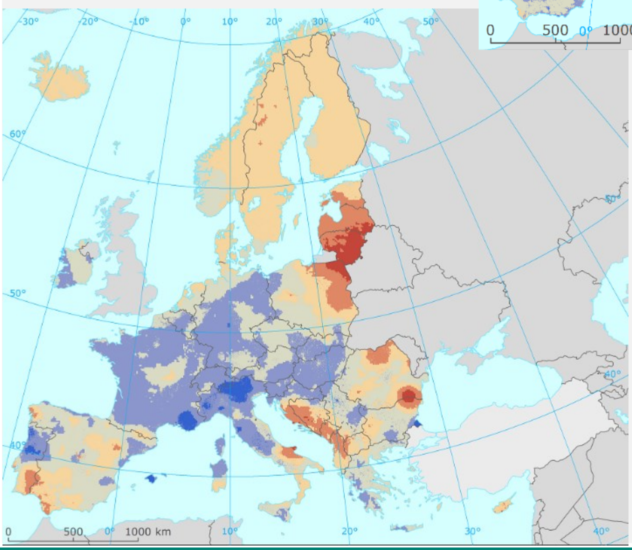

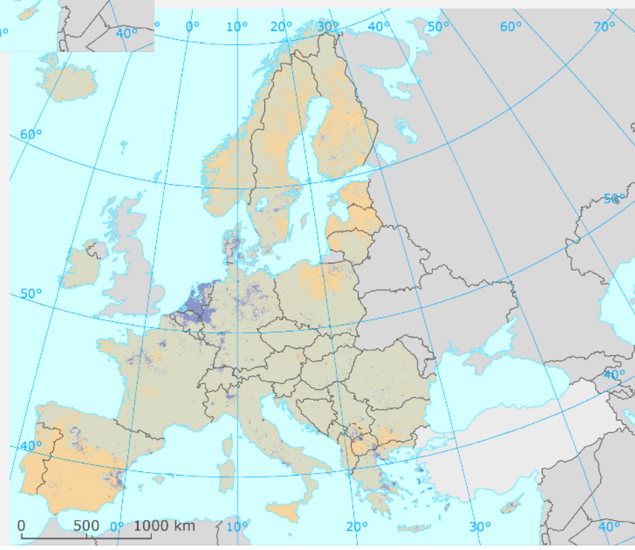

Authors:

Jan Horálek (CHMI), Leona Vlasáková (CHMI), Markéta Schreiberová (CHMI), Philipp Schneider (NILU), Nina Benešová (CHMI), Ondřej Vlček (CHMI)

European Environment Agency
European Topic Centre
Human health and the environment

Cover design: EEA
Cover image: Maps showing inter-annual differences in concentrations between 2022 and 2023 for $PM_{2.5}$ annual average (top), O_3 indicator peak season average of maximum daily 8-hour means (bottom left) and NO_2 annual average (bottom right). (This report´s Maps 4.2 right, 5.2 and 6.2 right.)
Layout: EEA / ETC HE (CHMI)

Publication Date: 26 November 2024
ISBN 978-82-93970-33-0

How to cite this report:
Horálek, J., Vlasáková, J., Schreiberová, M., Schneider, P., Benešová, N., Vlček, O. (2024). *Interim air quality maps of EEA member and cooperating countries for 2023. PM, O_3 and NO_2 spatial estimates* (Eionet Report – ETC HE 2024/1). European Topic Centre on Human Health and the Environment.

The report is available from https://www.eionet.europa.eu/etcs/all-etc-reports and https://zenodo.org/communities/eea-etc/?page=1&size=20.

EEA activity no. 3 Human Health and the Environment

ETC HE coordinator: Stiftelsen NILU, Kjeller, Norway (https://www.nilu.com/)

ETC HE consortium partners: Federal Environment Agency/Umweltbundesamt (UBA), Aether Limited, Czech Hydrometeorological Institute (CHMI), Institut National de l'Environnement Industriel et des Risques (INERIS), Swiss Tropical and Public Health Institute (Swiss TPH), Universitat Autònoma de Barcelona (UAB), Vlaamse Instelling voor Technologisch Onderzoek (VITO), 4sfera Innova S.L.U., klarFAKTe.U

More information on the European Union is available on the Internet (http://europa.eu).

European Topic Centre on
Human Health and the Environment (ETC HE)
https://www.eionet.europa.eu/etcs/etc-he

Contents

Acknowledgements

The ETC HE task manager was Jan Horálek (CHMI, Czechia). The EEA project manager was Alberto González Ortiz.

The external task ETC HE reviewer was Joana Soares (NILU, Norway).

There were other ETC HE contributions. The air quality monitoring data were extracted from the AQ e-reporting database by María Colina and Jaume Targa (4sfera, Spain). The data preparation and the analysis were assisted by Pavel Kurfürst and Jana Schovánková (CHMI, Czechia).

Summary

This report presents the interim air quality maps for the area of the member and cooperating countries of the European Environmental Agency (EEA) for the year 2023. These maps are based on the non-validated up-to-date measurement data and the CAMS Ensemble Forecast modelling results, together with other supplementary data.

The interim maps and further assessment present the annual average particulate matter (both PM_{10} and $PM_{2.5}$) concentration, the annual average nitrogen dioxide (NO_2) concentration and the ground-level ozone (O_3) concentration (in terms of peak season average of maximum daily 8-hour means).

The share of population living in the considered (i.e. presented) European area exposed to annual average PM_{10} concentration above the limit value (LV) of 40 µg/m^3 is estimated to be 0.1 %; for the EU-27, no population is estimated to be exposed to LV exceedances. Almost 60 % of both considered European and EU-27 populations have been exposed to annual average concentrations above the WHO Air Quality Guideline level of 15 µg/m^3. The population-weighted concentration of the PM_{10} annual average for 2023 for both considered European countries and for EU-27 is estimated to be about 17 µg/m^3. The population-weighted concentration of the PM_{10} annual averages shows quite a steady decrease of about 0.6 µg/m^3 per year in the period 2005-2023, with the lowest concentration in this period being recorded in 2023.

It is estimated that 0.3 % of the population living in the considered (i.e. presented) European area has been exposed to concentrations above the EU annual limit value (LV) of 25 µg/m^3. For the EU-27, no population is estimated to be exposed to LV exceedances. About 97 % of the population living in both the considered European area and the EU-27 has been exposed to concentrations above the WHO Air Quality Guideline level of 5 µg/m^3. The population-weighted concentration of the $PM_{2.5}$ annual average for 2023 is estimated to be 10.3 µg/m^3 for the EEA member and cooperating countries and 10.2 µg/m^3 for the EU-27. Throughout the whole period 2005-2023, the $PM_{2.5}$ annual average concentrations show a quite steady decrease of about 0.5 µg/m^3 per year. Like in the case of PM_{10}, the last year 2023 (based on the interim data) gives the lowest results in the 19-year period.

Based on the interim map for 2023, it has been estimated that almost 100 % of the considered European population and almost 100 % of the EU-27 population lived in areas where the O_3 concentration was above the peak season average of maximum daily 8-hour means of 60 µg/m^3. The peak season is defined as the six consecutive months of the year with the highest six-month running-average O_3 concentration. The population-weighted concentration of the O_3 peak season average of maximum daily 8-hour means for 2023 for both the considered European and the EU-27 population is estimated to be about 90 µg/m^3.

The share of the population living in the considered European and the EU-27 areas exposed to annual average NO_2 concentration above the limit value (LV) of 40 µg/m^3 is estimated to be 0.1 %. Around 64 % of the population living in both the considered European area and the EU-27 has been exposed to concentrations above the WHO Air Quality Guideline level of 10 µg/m^3. The population-weighted concentration of the NO_2 annual average for 2023 for both areas is estimated to be about 13 µg/m^3. Population-weighted concentration for the NO_2 annual average shows a steady decrease of about 0.6 µg/m^3 per year in the period 2005-2023, with the lowest concentration in this period recorded in 2023.

1 Introduction

European wide air quality (AQ) annual maps have been routinely constructed under the ETC HE (and the previous consortia) since 2005 (Horálek, 2024b and references therein). The mapping methodology combines monitoring data, chemical transport model (CTM) results and other supplementary data using a linear regression model followed by kriging of the residuals produced from that model ('residual kriging'). Separate mapping layers (rural, urban background and urban traffic, where relevant) are created separately and subsequently merged together into the final map. In order to reflect the three steps applied, the methodology is called *Regression – Interpolation – Merging Mapping (RIMM)*. The regular maps (i.e. maps presented under the ETC's regular mapping reports, e.g. Horálek et al., 2024b) are based on the validated air quality monitoring data as stored in the EEA's AQ e-reporting database (in the so-called E1a data set), the modelling results and other supplementary data. Due to the time schedule of the production and availability of the validated AQ measurement data, the regular RIMM maps of a year Y are typically available in May of year Y+2. Thus, the regular 2023 maps based on the validated data will be available ca. in May 2025.

This report presents the interim air quality maps for 2023 for the area of the EEA member and cooperating countries[1] (and the three microstates of Andorra, Monaco and San Marino). These maps are based on the non-validated up-to-date (UTD) measurement data (as available in the E2a data set of the AQ e-reporting database) and the CAMS Ensemble Forecast modelling results, together with other supplementary data. The reason for the production of these interim maps is their earlier availability. The interim maps creation was previously developed and evaluated, and consequently the interim maps of PM_{10}, $PM_{2.5}$, NO_2 and ozone (O_3) were recommended for regular production, see Horálek et al. (2021a, 2021b, 2023b). In order to overcome an obstacle of data gaps of the E2a data in some areas, the use of so-called pseudo stations data in the areas with the lack of E2a stations are used, based on the regression relation between the E2a data from a year Y and the validated E1a data from a year Y-1, together with the ratio of the modelling results from years Y and Y-1. The use of the pseudo station data in the interim mapping is applied for PM_{10}, $PM_{2.5}$ and NO_2. For O_3, the data coverage of the E2a data is larger and the interim O_3 maps might be constructed without the use of the pseudo stations. The interim maps are not produced for the area of Türkiye, due to the lack of E2a monitoring data from Turkish stations.

In this report, interim 2023 maps for the PM_{10} annual average, the $PM_{2.5}$ annual average, the NO_2 annual average and the O_3 indicator peak season average of maximum daily 8-hour means are presented. Also, the difference between the five-year mean 2018-2022 (where available) and 2023 and the inter-annual difference between 2022 and 2023 are discussed. In addition, population exposure estimated based on the concentration maps is briefly shown. Based on the analysis presented in Horálek et al. (2023a), we provide in this report basic exposure estimates only, not the detailed information for individual countries. The exposure estimates are presented for five large European regions (Northern Europe, Western Europe, Central Europe, Southern Europe and South-Eastern Europe), for the EU-27 and for the whole mapping area. Apart from this, the evolution of the overall population-weighted concentration in the 19-year period 2005-2023 is also shown, where available.

Apart from the 2023 interim maps, this report also presents the validation of the interim maps for 2022 as presented in Horálek et al. (2023b), based on the validated E1a data for 2022. It also presents the

([1]) The EEA member countries are the 27 Member States of the European Union (EU-27), Iceland, Lichtenstein, Norway, Switzerland, and Türkiye. The EEA cooperating countries are Albania, Bosnia and Herzegovina, Montenegro, North Macedonia, Serbia, and Kosovo under the UN Security Council Resolution 1244/99. In this report, Kosovo is considered individually, without prejudice on its status.

comparison of the exposure tables based on the interim maps for 2022 (Horálek et al., 2023b) against the exposure tables based on the regular maps (Horálek et al., 2024b).

Chapters 2, 3, and 4 present the concentration maps and basic exposure estimates for particulate matter, O_3 and NO_2, respectively. Chapter 5 brings the conclusions. Annex 1 describes briefly the methodological aspects (including the geographical distribution of the considered area into five large regions) and Annex 2 presents the input data applied. Annex 3 provides the technical details of the maps and their uncertainty estimates. Annex 4 provides the validation of the interim maps and exposure estimates for 2022.

2 Particulate matter

2.1 PM_{10} annual average

Map 2.1 presents the interim map for the PM_{10} annual average 2023, as the result of interpolation and merging of the separate map layers as described in Annex 1 Section A1.1 (for technical details of this map, see Annex 3, Section A3.1). Red and dark red areas indicate concentrations above the EU annual limit value (LV) of 40 µg/m^3 (EC, 2008). Green areas show concentrations below the revised EU annual LV of 20 µg/m^3 (LV_{2030}, to be attained by 2030). Dark green indicates the areas where the PM_{10} annual average concentration is below the WHO Air Quality Guideline (AQG) level of 15 µg/m^3 (WHO, 2021).

Map 2.1: Interim concentration map of PM_{10} annual average, 2023

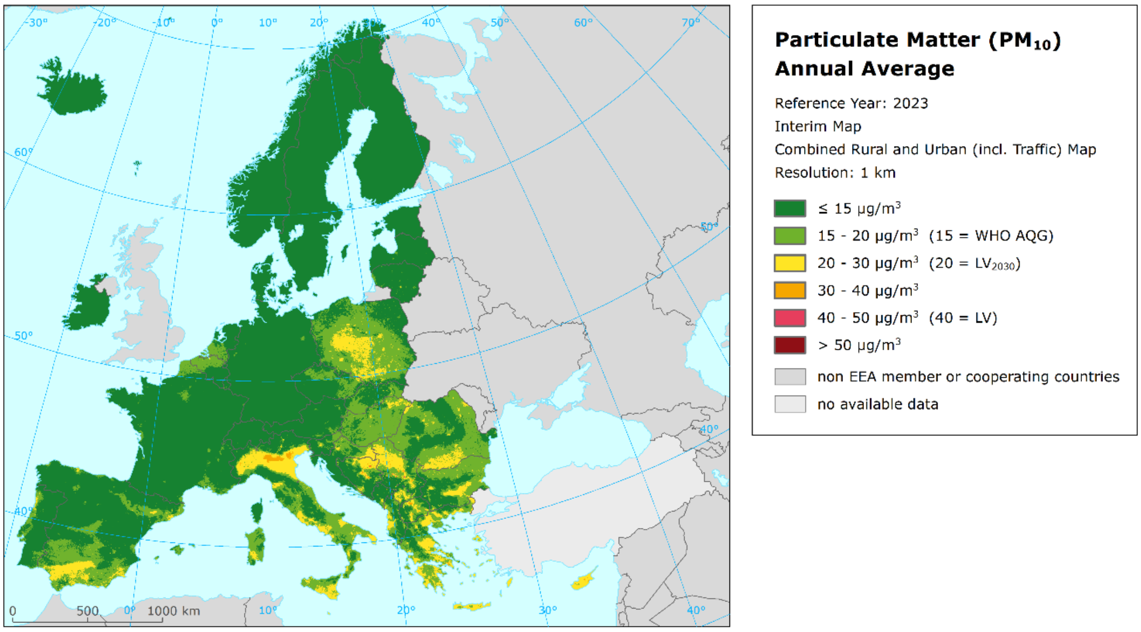

The map shows concentrations above the annual LV only in urban areas around some Balkan cities (in Bosnia and Herzegovina, North Macedonia and Serbia). In addition to these countries, there are areas in the Po Valley, in Italy, and smaller disconnected areas in Bosnia and Herzegovina, Serbia, Albania, North Macedonia, Bulgaria, Greece and Cyprus where PM_{10} concentrations of 30-40 µg/m^3 have been estimated. Most of Europe show concentrations below 20 µg/m^3, with concentrations below 15 µg/m^3 estimated for most of western (except parts of the Île de France region, Benelux, Spain and Portugal) and northern Europe.

The relative mean uncertainty (Relative RMSE) of this map is 19 % for rural and 18 % for urban background areas (Annex 3, Table A3.2). However, these uncertainty estimates are based on the non-validated E2a data and are valid only for areas covered by the E2a stations. The complete validation of the interim PM_{10} map can only be done when the validated E1a data for 2023 are available. For such validation of the interim PM_{10} map for 2022 as presented in Horálek et al. (2023b), see Annex 4, Section A4.1.

Map 2.2 shows the difference between the five-year mean 2018-2022 and 2023 and the inter-annual difference between 2022 and 2023 (using the regular maps for 2018-2022 and the 2023 interim map) for PM_{10} annual average. Orange to red areas show an increase of PM_{10} concentration in 2023, while blue areas show a decrease.

Compared to the five-year mean 2018-2022, the highest increases in annual mean PM_{10} concentrations (> 5 µg/m^3) are observed mainly in parts of Greece and Cyprus. Increases > 2 µg/m^3 are observed in parts of southern and south-eastern Europe (parts of Spain, southern France, parts of Italy, Bosnia and Herzegovina, Bulgaria, North Macedonia, Greece and Cyprus). On the other hand, relatively continuous areas of central and south-eastern Europe show a decrease in annual average PM_{10}, with the deepest decreases in parts of Poland, Bulgaria and Spain. No change or slight increases/decreases of about 2 µg/m^3 are observed in most of Europe (France, parts of central Europe, parts of south-eastern Europe and parts of northern Europe).

Based on the map of the inter-annual difference between 2022 and 2023, there is no change or only slight increases or decreases (i.e. ±2 µg/m^3) in annual average PM_{10} concentrations in almost the entire considered (i.e. presented) European area. Nevertheless, increases in concentrations are particularly evident in Greece and in a few parts of other Balkan states. Decreases in concentrations have been observed mainly in parts of Poland, Germany, Italy, France, Spain and Portugal.

Map 2.2: Difference in concentrations between five-year mean 2018-2022 (left) or 2022 (right) and 2023 (based on the interim map) for PM_{10} annual average

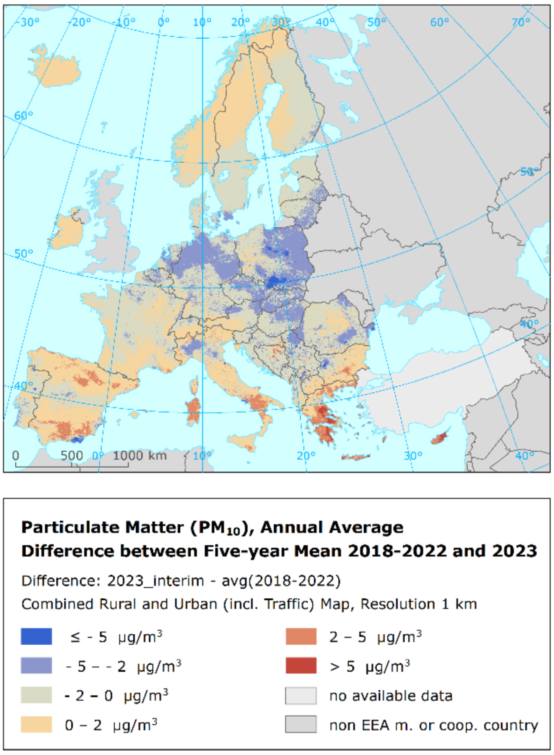

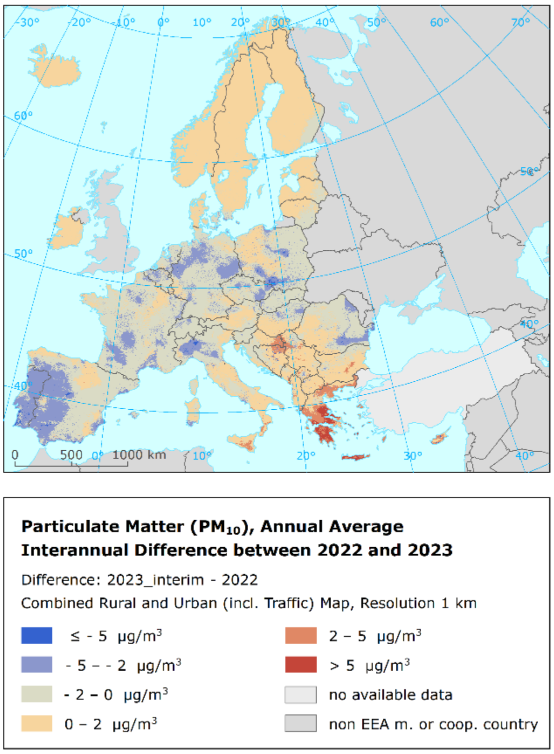

Based on the mapping results and the population density data, the population exposure estimates have been calculated. Table 2.1 gives the population frequency distribution for a limited number of exposure classes and the population-weighted concentration for five large European regions, for EU-27 and for the total presented area. The exposure estimate for individual countries is not presented, due to their high uncertainty. As presented in Horálek et al. (2023a), the exposure estimates based on interim maps give good results for the total area and the EU-27, but somewhat poorer results for individual countries.

Based on the interim map, it is estimated that 0.1 % of the population living in the considered (i.e. presented) European area has been exposed to concentrations above the EU annual limit value (ALV) of 40 µg/m³. Most of them live in south-eastern Europe, where the share is about 1 %. All of them live outside EU-27. Almost 60 % of both the considered European and the EU-27 population has been exposed to annual average concentrations above the WHO Air Quality Guideline level of 15 µg/m³ (WHO, 2021). The population-weighted concentration of the PM_{10} annual average for 2023 both for the considered European countries and for EU-27 is estimated to be about 17 µg/m³.

Table 2.1: Population exposure and population-weighted concentration, PM_{10} annual average, 2023, based on the interim map

Area	Population [inhbs·1000]	PM_{10} – annual average, exposed population, 2023 [%]						PM_{10} ann. avg.
		< 15 µg/m³	15-20 µg/m³	20-30 µg/m³	30-40 µg/m³	40-50 µg/m³	> 50 µg/m³	Pop. weighted [µg/m³/inhbs]
Northern Europe	34 055	90.4	8.7	0.9				10.7
Western Europe	86 258	55.8	42.6	1.6				14.7
Central Europe	167 045	58.6	26.9	14.4	0.0			15.3
Southern Europe	142 486	14.2	34.8	46.8	4.2			20.4
South-eastern Europe	46 106	6.0	33.9	51.5	7.5	1.2		22.2
Total	**475 951**	**41.6**	**31.5**	**24.7**	**2.0**	**0.1**		**17.1**
EU-27	**444 258**	**41.4**	**33.0**	**24.1**	**1.4**	**0.0**		**17.0**

Note: The percentage value "0.0" indicates that an exposed population exists, but it is small and estimated to be less than 0.05 %. Empty cells mean no population in exposure.

Figure 2.1 shows, for the whole considered area, the population frequency distribution for exposure classes with a width of 1 µg/m³. The highest population frequency is found for classes between 12 and 18 µg/m³. A quite continuous decline of the population frequency is visible for classes between 20 and 30 µg/m³ and beyond 35 µg/m³.

Figure 2.1: Population frequency distribution, PM_{10} annual average 2023, based on the interim map. The WHO AQG level (15 µg/m³) is marked by the green line, the revised EU annual LV_{2030} (20 µg/m³) is marked by the yellow line, the EU annual LV (40 µg/m³) is marked by the red line.

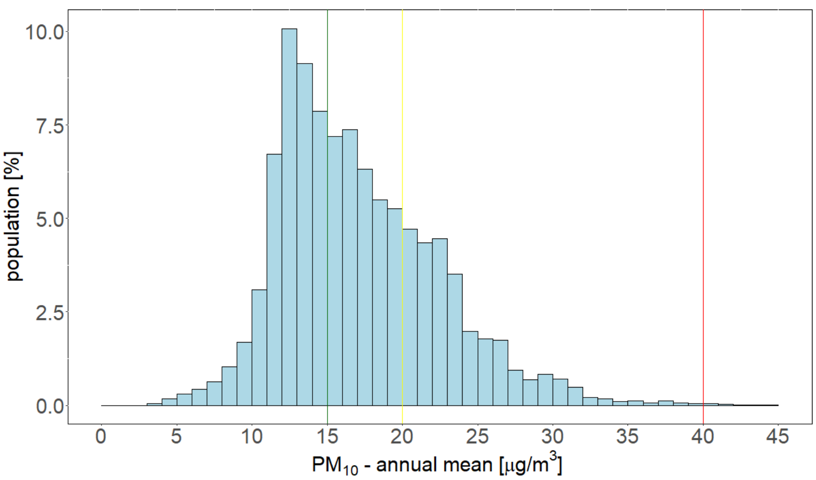

For changes in the population-weighted concentration of the PM_{10} annual average in the 19-year period 2005-2023, see Figure 2.2. For the previous years, mapping results as presented in Horálek et al. (2024b and references therein) have been used. Since the 2017 results were calculated in 2019, PM_{10} maps were prepared based on the updated method (taking into account air quality in urban traffic areas). Furthermore, the updated method was also used to remap years 2005, 2009 and 2015-2016. For comparability reasons, results for 2005, 2009 and 2015-2019 are presented in two variants, i.e. based on both the old and the updated methodologies. Another issue is that for the 16-year time series 2005-2020, the overall population-weighted mean included the United Kingdom. Therefore, for consistency reasons, the population-weighted concentration for the whole area, including the United Kingdom, is presented also for 2021-2023. This value was easily available, as the mapping domain includes the United Kingdom (see Section 2.1).

Figure 2.2: Population-weighted concentration of the PM_{10} annual average in 2005-2023, based on both the old (blue) and the updated (red) mapping methodology (where available), and with interim results for the year 2023

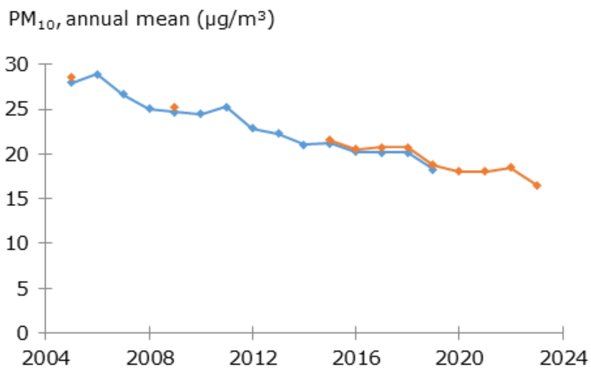

Throughout the whole period 2005-2023, the PM_{10} annual average concentrations show a quite steady decrease of about 0.6 μg/m^3 per year. One can see that the last year, 2023 (based on the interim data), is estimated to have the lowest concentrations in the 19-year period.

2.2 $PM_{2.5}$ annual average

Map 2.3 presents the interim map for the $PM_{2.5}$ annual average 2023, as the result of interpolation and merging of the separate map layers as described above (for technical details of this map, see Annex 3, Section A3.2). Dark red areas show concentrations above the EU annual limit value (LV) of 25 μg/m^3 (EC, 2008). Red areas show concentrations above the indicative LV of 20 μg/m^3 defined as Stage 2 (ILV). Yellow areas indicate concentrations above the revised EU annual LV of 10 μg/m^3 (LV_{2030}, to be attained by 2030). Dark green indicates the areas where the $PM_{2.5}$ annual average concentration is below the WHO Air Quality Guideline (AQG) level of 5 μg/m^3 (WHO, 2021).

The map shows $PM_{2.5}$ concentrations above the annual LV in some scattered urban areas of Bosnia and Herzegovina North Macedonia, and Serbia. Concentrations above the ILV appear in the Po Valley (in northern Italy), in the Krakow – Katowice (Poland) – Ostrava (Czechia) industrial region, in the areas of central Serbia and in some scattered areas of central and south-eastern Europe and Greece. In central and south-eastern Europe, areas with concentrations of 10-15 μg/m^3 as well as 5-10 μg/m^3 can be found. In southern Europe, concentrations mostly fall within the 5-10 μg/m^3 range, with some areas (parts of the Iberian Peninsula, parts of France, and northern Italy) showing concentrations below 5 μg/m^3 (i.e. WHO AQG). In northern Europe, concentrations are predominantly below 5 μg/m^3.

The relative mean uncertainty (RRMSE) of this map is 19 % for rural areas and 21 % for urban background areas (Annex 1). However, these uncertainty estimates are based on the non-validated E2a data and are valid only for areas covered by the E2a stations. The complete validation of the interim $PM_{2.5}$ map can only be done when the validated E1a data for 2023 are available. For such validation of the interim $PM_{2.5}$ map for 2022 as presented in Horálek et al. (2023b), see Annex 2, Section A2.1.

Map 2.3: Interim concentration map of $PM_{2.5}$ annual average, 2023

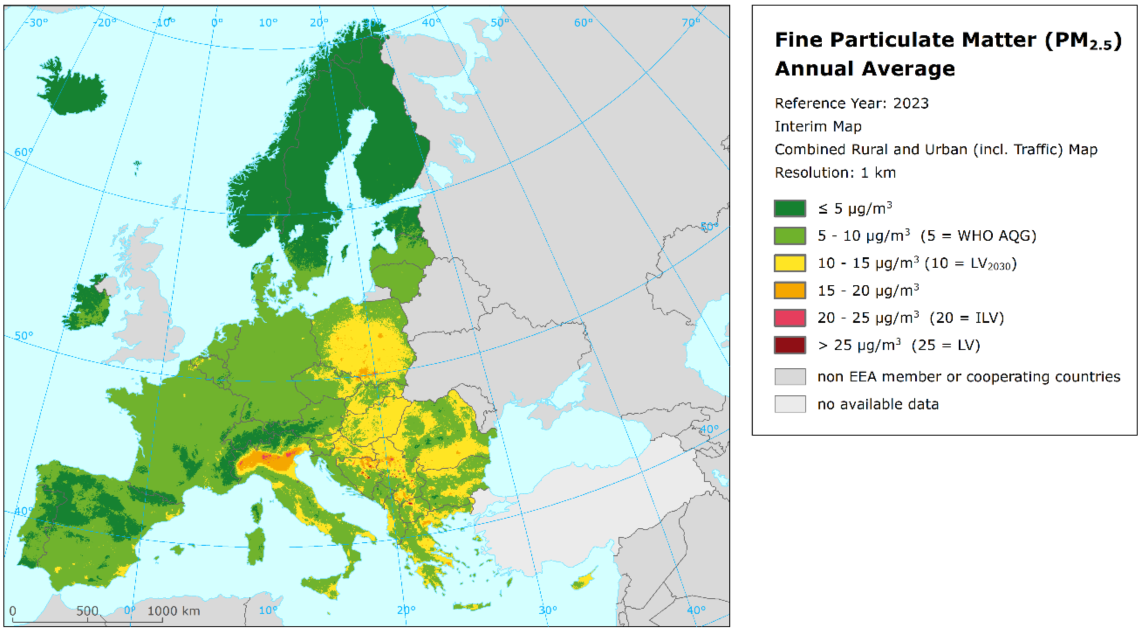

Map 2.4 shows the difference between the five-year mean 2018-2022 and 2023 and the inter-annual difference between 2022 and 2023 (using the regular maps for 2018-2022 and the 2023 interim map) for the $PM_{2.5}$ annual average. Orange to red areas show an increase of $PM_{2.5}$ concentration in 2023, while blue areas show a decrease.

Compared to the five-year average from 2018 to 2022, no changes or only slight increases or decreases (±1.5 µg/m³) in annual average $PM_{2.5}$ concentrations were observed across most of western, southern, and northern Europe, as well as in large parts of south-eastern Europe. A more notable decrease was recorded in central Europe, with the highest decrease seen in the Krakow–Katowice (Poland)–Ostrava (Czechia) region.

Based on the map of the inter-annual difference between 2022 and 2023, there is no change or only slight increases or decreases in annual average $PM_{2.5}$ concentrations across most of the considered (i.e. presented) European area. Noticeable increases are particularly evident in parts of Greece, while decreases have been observed primarily in Poland and Romania and in parts of other countries, including Portugal, Spain, Italy, Czechia, Hungary, and Bulgaria.

Map 2.4: Difference in concentrations between five-year mean 2018-2022 (left) or 2022 (right) and 2023 (based on the interim map) for $PM_{2.5}$ annual average

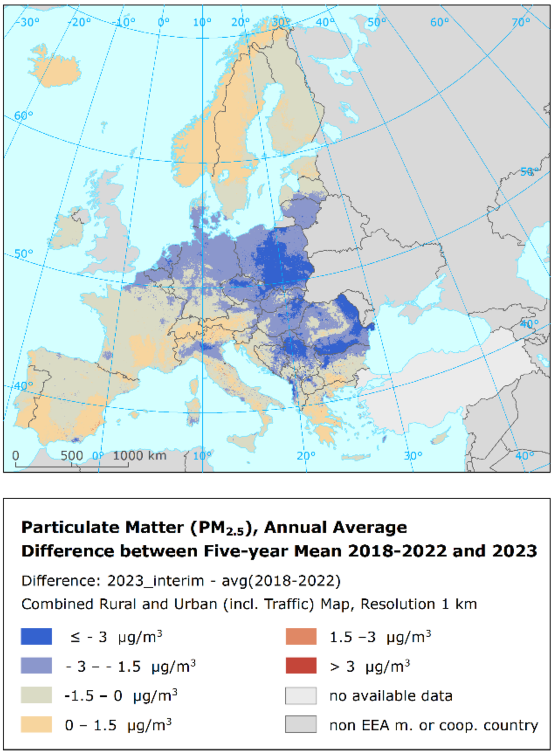

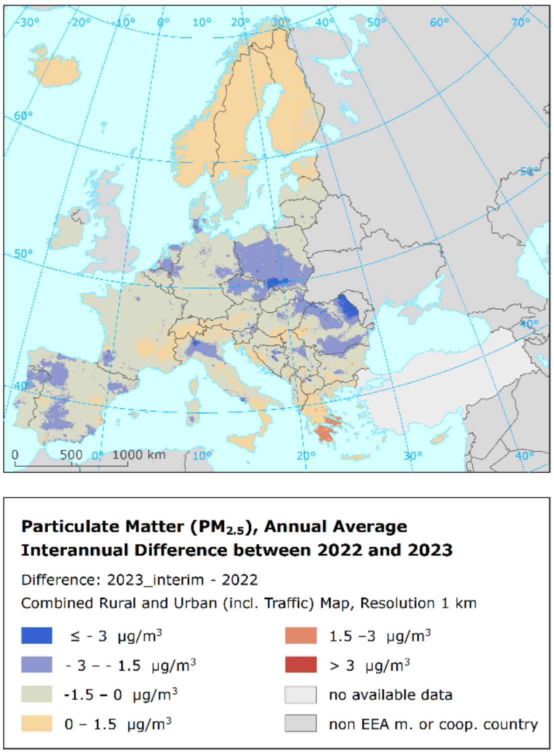

Based on the mapping results and the population density data, the population exposure estimates have been calculated. Table 2.2 gives the population frequency distribution for a limited number of exposure classes and the population-weighted concentration for large European regions, for EU-27 and for the total presented area.

Table 2.2: Population exposure and population-weighted concentration, $PM_{2.5}$ annual average, 2023, based on the interim map

Area	Population [inhbs·1000]	$PM_{2.5}$ – annual average, exposed population, 2023 [%]						$PM_{2.5}$ ann. avg.
		< 5 µg/m³	5-10 µg/m³	10-15 µg/m³	15-20 µg/m³	20-25 µg/m³	> 25 µg/m³	Pop. weighted [µg/m³/inhbs]
Northern Europe	34 055	35.2	63.3	1.5				5.8
Western Europe	86 258	1.4	91.4	7.2				8.3
Central Europe	167 045	0.2	62.0	28.3	9.1	0.4		10.1
Southern Europe	142 486	1.1	43.2	38.9	14.1	2.7		11.3
South-eastern Europe	46 106	0.0	8.7	50.7	29.2	8.4	3.0	14.7
Total	**475 951**	**3.1**	**56.2**	**28.2**	**10.4**	**1.8**	**0.3**	**10.3**
EU-27	**444 258**	**2.7**	**57.5**	**29.0**	**9.7**	**1.0**		**10.2**

Note: The percentage value "0.0" indicates that an exposed population exists, but it is small and estimated to be less than 0.05 %. Empty cells mean no population in exposure.

Based on the interim map, it is estimated that 0.3 % of the population living in the considered (i.e. presented) European area has been exposed to concentrations above the EU annual limit value (LV) of 25 µg/m³. For the EU-27, no population is estimated to be exposed to LV exceedances. About 97 % of the population living in both the considered European area and the EU-27 has been exposed to concentrations above the WHO Air Quality Guideline level of 5 µg/m^3. The population-weighted concentration of the $PM_{2.5}$ annual average for 2023 is estimated to be about 10 µg/m^3 for both the all considered countries and the EU-27.

Figure 2.3 shows, for the whole considered area, the population frequency distribution for exposure classes with a width of 0.5 µg/m^3. The highest population frequency is found for classes between 7 and 12 µg/m^3. A quite continuous decline of the population frequency can be seen for population classes beyond 12 µg/m^3.

Figure 2.3: Population frequency distribution, $PM_{2.5}$ annual average, 2023, based on the interim map. The WHO AQG level (5 µg/m^3) is marked by the green line, the revised EU annual LV_{2030} (10 µg/m^3) is marked by the yellow line, the EU annual indicative LV (20 µg/m^3) is marked by the orange line and the EU annual LV (25 µg/m^3) is marked by the red line.

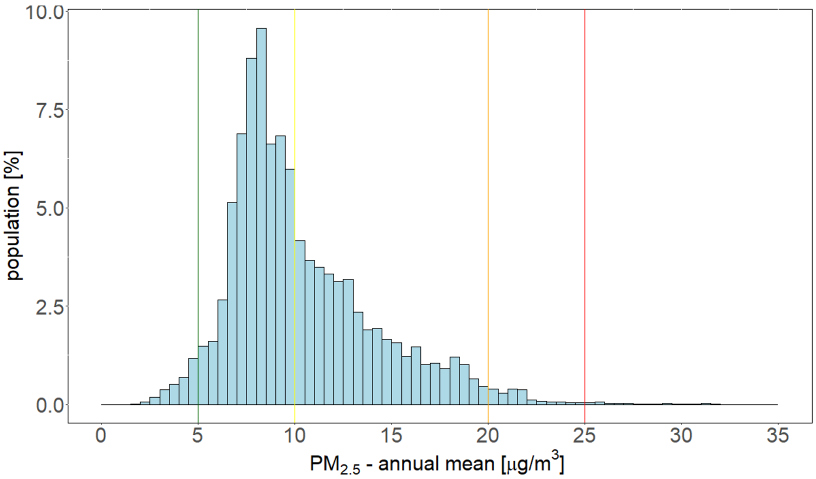

For changes in the population-weighted concentration of the $PM_{2.5}$ annual average in the 19-year period 2005-2023, see Figure 2.4. For the previous years, mapping results as presented in Horálek et al. (2024b and references therein) have been used. Since the 2017 results were estimated in 2019, $PM_{2.5}$ maps were prepared based on the updated method (taking into account air quality in urban traffic areas). Furthermore, the updated method was also used to remap years 2005, 2009 and 2015-2016. For comparability reasons, results for 2005, 2009 and 2015-2019 are presented in two variants, i.e. based on both the old and the updated methodologies. Like PM_{10}, the population-weighted concentration for the whole area, including the United Kingdom, is presented for the whole period for consistency.

Figure 2.4: Population-weighted concentration of the $PM_{2.5}$ annual average in 2005-2023, based on both the old (blue) and the updated (red) mapping methodology (where available), and with interim results for the year 2023

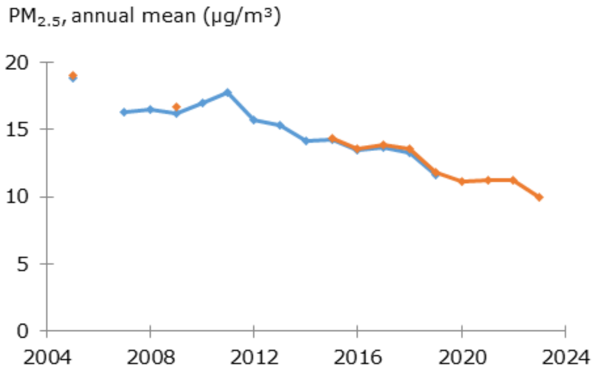

Throughout the whole period 2005-2023, the $PM_{2.5}$ annual average concentrations show a quite steady decrease of about 0.5 µg/m^3 per year. Like in the case of PM_{10}, the last year, 2023 (based on the interim data), is estimated to have the lowest estimates in the presented period.

3 Ozone

3.1 O_3 – peak season average of maximum daily 8-hour means

In September 2021, the WHO introduced new AQG for O_3. The new long-term Air Quality Guideline (AQG) level for O_3 is set at 60 µg/m³, expressed as the average of daily maximum 8-hour mean O_3 concentration of the so-called peak season. The peak season is defined as the six consecutive months of the year with the highest six-month running-average O_3 concentration (WHO, 2021).

Map 3.1 presents the interim 2023 map for the O_3 indicator peak season average of maximum daily 8-hour means. The map is a result of merging separate rural and urban interpolated map layers as described in Annex 1 Section A1.1 (for technical details of this map, see Annex 3, Section A3.3). Red and purple areas show values above 100 µg/m³, while the dark green show areas where the values of the peak season indicator are below the WHO Air Quality Guideline level of 60 µg/m³ (WHO, 2021). Generally, southern Europe shows higher concentrations of the O_3 peak season indicator than northern Europe.

Map 3.1: Interim concentration map of O_3 indicator peak season average of maximum daily 8-hour means, 2023

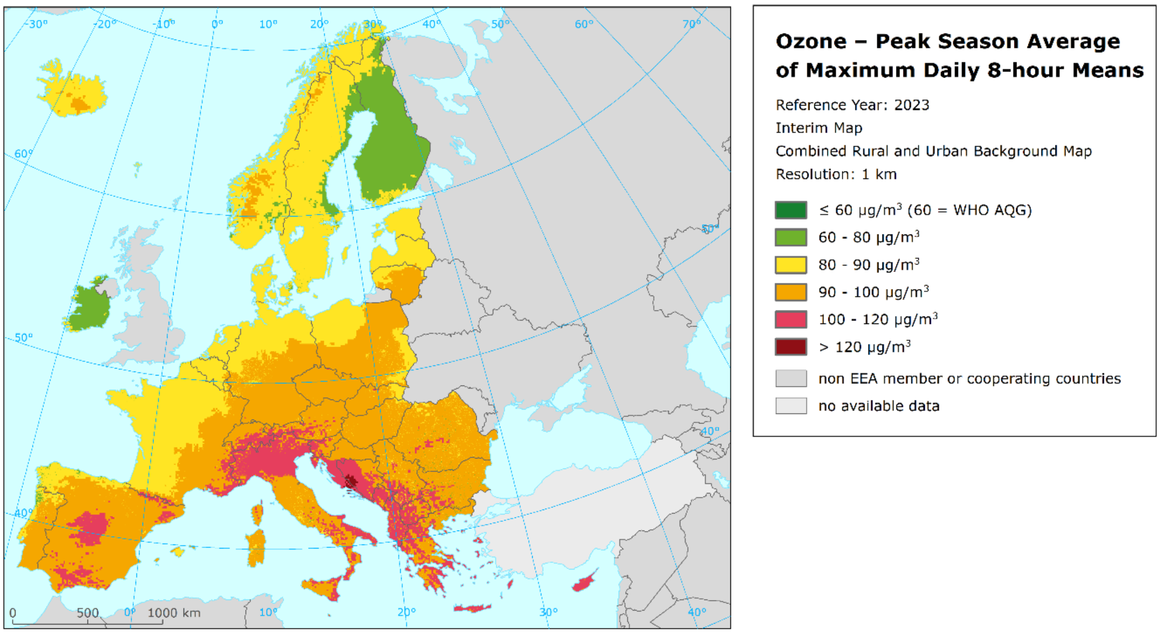

The map shows that in 2023 areas with a peak season average of maximum daily 8-hour means exceeding 60 µg/m³ cover almost the entire considered region. Lower values (< 90 µg/m³) are observed in northern Europe (Sweden, Finland, the Baltic states, Iceland), as well as in Ireland, northern Poland, Germany, the Benelux countries, in a large area of France, and in many urban areas of the south-eastern Europe. Higher values (> 100 µg/m³) are recorded in northern Italy, central Spain, and various parts of the Balkan states and Cyprus.

The relative mean uncertainty (RRMSE) of this map is 36 % for rural and 37 % for urban background areas (Annex 3, Table A3.5). However, these uncertainty estimates are based on the non-validated E2a data and are valid only for areas covered by the E2a stations. The complete validation of the interim O_3 map can only be done when the validated E1a data for 2023 are available.

Map 3.2 shows the inter-annual difference between 2023 and 2022 for the O_3 indicator peak season average of maximum daily 8-hour means. Orange to red areas show an increase in O_3 concentration in 2023, while blue areas show a decrease.

Compared to 2022, most regions in Scandinavia, Ireland, central Europe, Spain, Italy, and south-eastern Europe experienced no significant changes or only slight variations (±4 µg/m³) in the O_3 peak season average of maximum daily 8-hour means. A noticeable increase in the O_3 peak season average is observed in the Baltic countries, northern and eastern Poland, and parts of Portugal and the Balkan region. Conversely, a decrease is evident in large areas of France, Germany, Italy, Slovenia, Portugal, Hungary, Slovakia, and various parts of the Balkans.

Map 3.2: Difference in concentrations between 2022 and 2023 (based on the interim map) for O_3 indicator peak season average of maximum daily 8-hour means

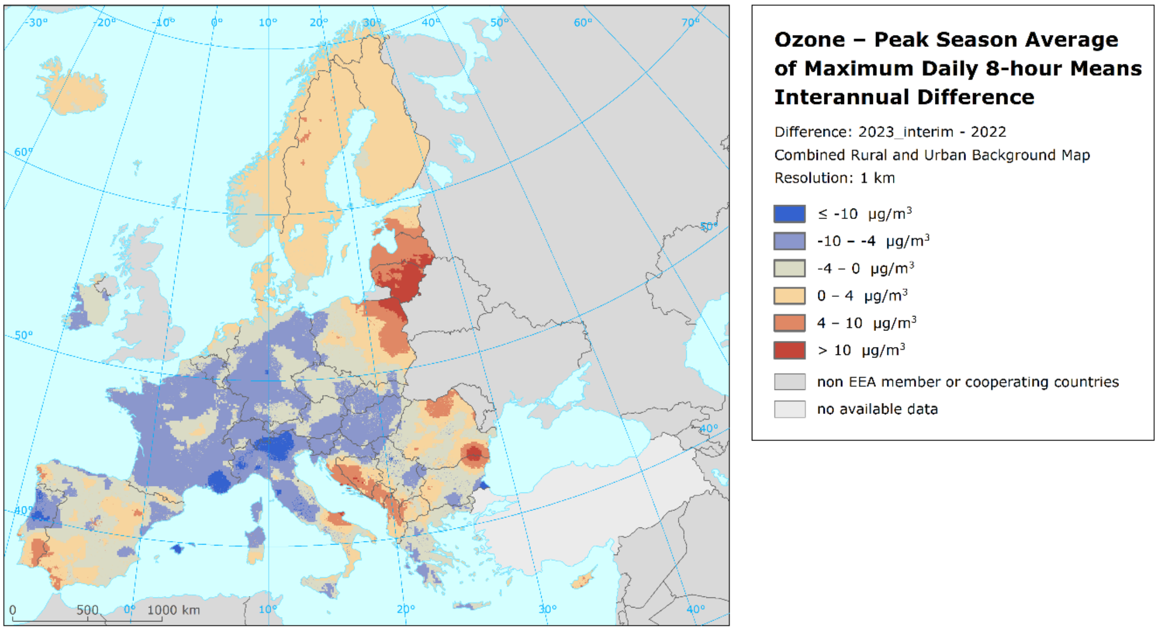

Based on the mapping results and the population density data, the population exposure estimate has been calculated. Table 3.1 gives the population frequency distribution for a limited number of exposure classes and the population-weighted concentration for large European regions, for EU-27 and for the total mapping area. The exposure estimate for individual countries is not presented, due to their high uncertainty. As presented in Horálek et al. (2023a), the exposure estimates based on interim maps give good results for the total area and the EU-27, but somewhat poorer results for individual countries.

Based on the interim map for 2023, it has been estimated that almost 100 % of the considered European population and almost 100 % of the EU-27 population lived in areas where the O_3 concentration was above the peak season average of maximum daily 8-hour means of 60 µg/m³. The population-weighted concentration of the O_3 peak season average of maximum daily 8-hour means for 2023 for both the considered European and the EU-27 population is estimated to be 90 µg/m³.

Table 3.1: Population exposure and population-weighted concentration, O_3 indicator peak season average of maximum daily 8-hour means, 2023, based on an interim map

Area	Population [inhbs·1000]	O_3 – peak season indicator, exposed population, 2023 [%]						O_3 – peak s. indic.
		< 60 µg/m³	60 -80 µg/m³	80 -90 µg/m³	90 -100 µg/m³	100 -120 µg/m³	> 120 µg/m³·d	Pop. weighted [µg/m³inhbs]
Northern Europe	34 055		49.7	45.2	5.1			81.2
Western Europe	86 258		6.8	80.2	13.1	0.0		85.5
Central Europe	167 045			43.3	56.4	0.3		90.6
Southern Europe	142 486	0.0	7.3	24.2	40.4	28.0		94.3
South-eastern Europe	46 106	0.3	21.2	44.2	27.5	6.0	0.7	86.6
Total	**475 951**	**0.0**	**9.0**	**44.3**	**37.4**	**9.1**	**0.1**	**89.7**
EU-27	**444 258**	**0.1**	**8.4**	**45.2**	**37.0**	**9.3**	**0.1**	**89.8**

Note: The percentage value "0.0" indicates that an exposed population exists, but it is small and estimated to be less than 0.05 %. Empty cells mean no population in exposure.

Figure 3.1 shows, for the whole considered area, the frequency distribution of the O_3 peak season average of maximum daily 8-hour means for population exposure classes of 1 µg/m^3. The highest population frequency is found for classes between ca 85 and 95 µg/m^3. For classes above 95 µg/m^3, a sharp decline of the population frequency can be seen.

Figure 3.1: Population frequency distribution, O_3 indicator peak season average of maximum daily 8-hour means, 2023, based on the interim map. The WHO AQG level (60 µg/m^3) is marked by the green line.

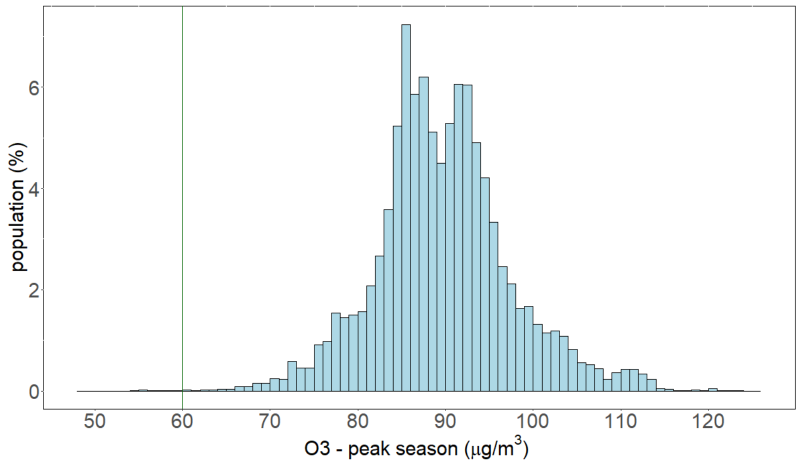

The map of the O_3 peak season indicator has been prepared for the second year only, so no evolution in a longer period can be shown.

4 Nitrogen dioxide

4.1 NO_2 annual average

Map 4.1 presents the interim map for the NO_2 annual average 2023, as the result of interpolation and merging of the separate map layers as described in Annex 1 Section A1.1 (for technical details of this map, see Annex 3, Section A3.4). Red and purple areas indicate concentrations above the annual limit value (LV) of 40 µg/m^3 (EC, 2008). Green areas show concentrations below the new EU annual LV of 20 µg/m^3 (LV$_{2030}$, to be attained by 2030). Dark green areas indicate concentrations below 10 µg/m^3, being the WHO Air Quality Guideline level (WHO, 2021).

According to Map 4.1, no areas where NO_2 concentrations exceeded the annual limit value (ALV) of 40 µg/m^3 were observed. (Note that in the traffic map layer there are some small urban traffic areas with NO_2 values above ALV that are smoothed in the 1 km resolution combined map and therefore not shown in that combined final map., as explained in the paragraph below). Moreover, some cities, such as Athens, Bucharest, Madrid, Milan, Paris, and Rome show NO_2 levels above 30 µg/m^3. The urbanized areas of several major cities, including Belgrade, Budapest, Naples, Sofia, and Warsaw, fall within the range of annual average NO_2 concentrations between 20 and 30 µg/m^3. Most of Europe shows NO_2 levels below AQG of 10 µg/m^3, while a larger region with concentrations between 10 and 20 µg/m^3 is found in the Po Valley.

It should be noted that the interpolated map is created at 1 km resolution only. Although the urban traffic map layer is used in the map creation, the traffic locations are smoothed in the final map at 1 km resolution. Thus, the map as such refers to the rural and urban background situations, while the values above the NO_2 ALV occur mostly at local hotspots such as dense traffic locations. Such concentrations (although occurred at some urban traffic locations in 2023) are not visible in the 1 km resolution Map 4.1.

Map 4.1: Interim concentration map of NO_2 annual average, 2023

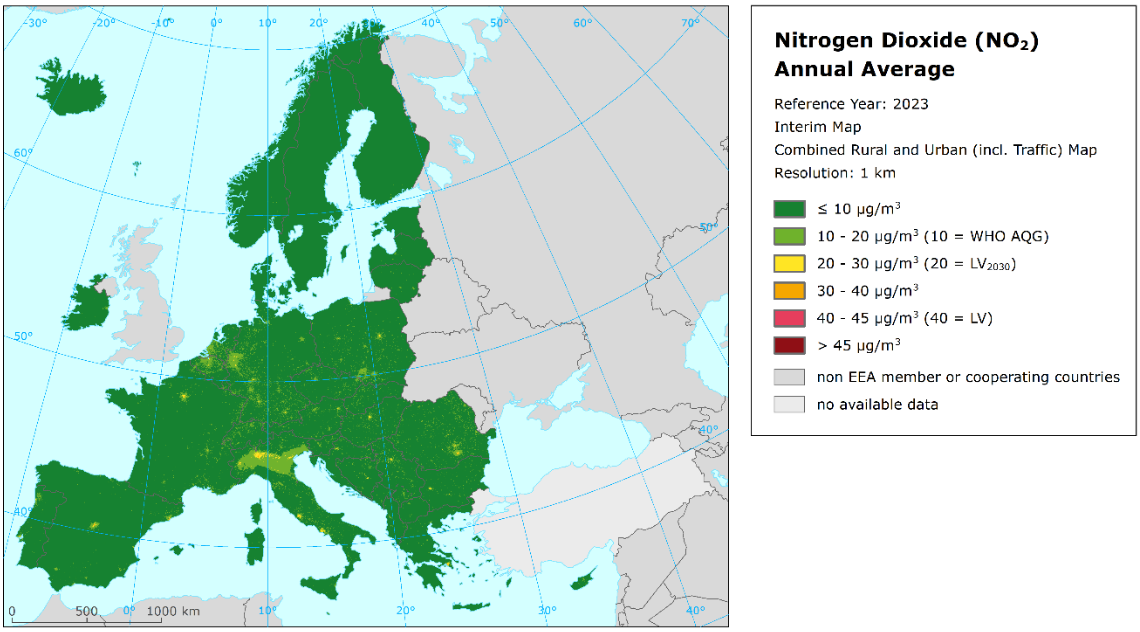

The relative mean uncertainty (RRMSE) of this map is 31 % for rural areas and 25 % for urban background areas (Annex 3, Table A3.7). However, these uncertainty estimates are based on the non-validated E2a data and are valid only for areas covered by the E2a stations. The complete validation of the interim NO_2 map can only be done when the validated E1a data for 2023 are available. For such validation of the interim NO_2 map for 2022 as presented in Horálek et al. (2023b), see Annex 2, Section A2.1.

Map 4.2 shows the difference between five-year mean 2018-2022 and 2023 and the inter-annual difference between 2022 and 2023 (using the regular maps for 2018-2023 and the 2023 interim map) for the NO_2 annual average. Orange to red areas show an increase of NO_2 concentration in 2023, while blue areas show a decrease.

Compared to the five-year mean 2018-2022, no increases in annual mean NO_2 concentrations above 2 µg/m^3 are seen. On the other hand, relatively continuous areas in Denmark, Benelux and Germany show a decrease in annual average NO_2 bigger than 2 µg/m^3. No change or slight increases/decreases of about 2 µg/m^3 are observed in almost the entire considered (i.e. presented) European area.

Based on the map of the inter-annual difference between 2022 and 2023, there is no change or a slight increase/decrease (±2 µg/m^3) in annual average NO_2 concentrations in almost the entire considered (i.e. presented) European area. No increases in concentrations above 2 µg/m^3 are evident. Decreases in concentrations have been observed mainly in the Benelux region and in many fragmented smaller parts in Denmark, France, Germany, Spain, Italy and some of the Balkan states.

Map 4.2: Difference in concentrations between five-year mean 2018-2022 (left) or 2022 (right) and 2023 (based on the interim map) for NO_2 annual average

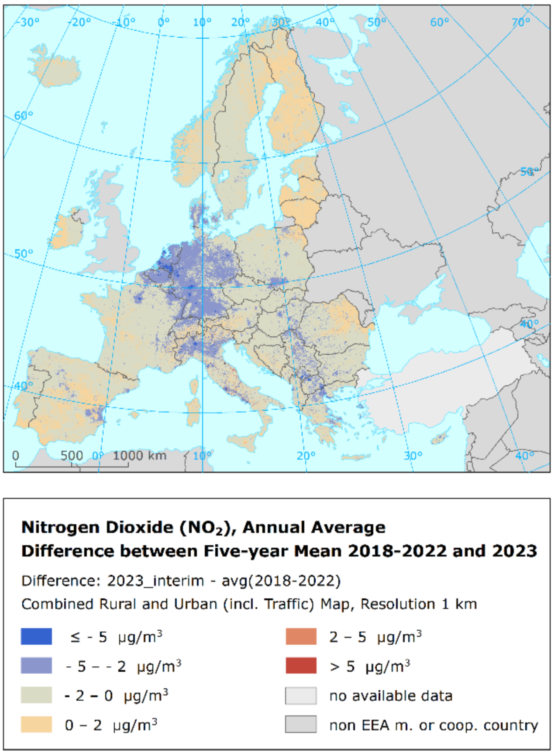

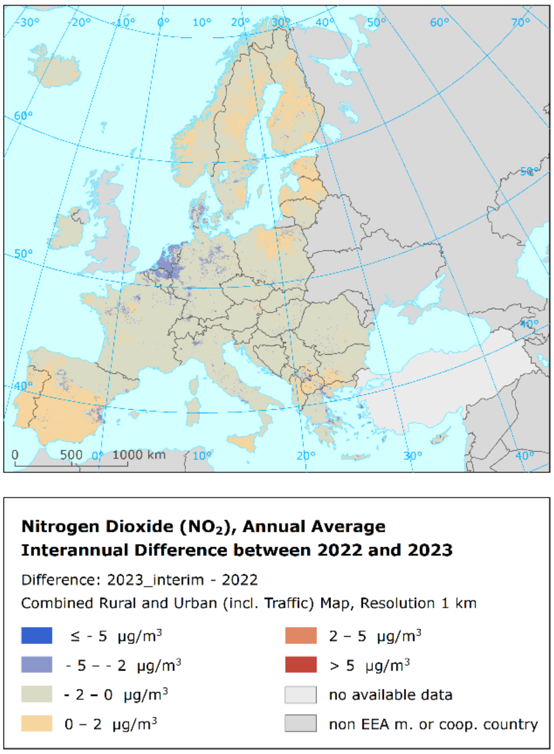

Based on the mapping results and the population density data, the population exposure estimate has been calculated. Table 4.1 gives the population frequency distribution for a limited number of exposure classes and the population-weighted concentrations for large European regions, for EU-27 and for the total mapping area. The exposure estimates for individual countries are not presented, due to their high uncertainty. As presented in Horálek et al. (2023a), the exposure estimates based on interim maps give good results for the total area and the EU-27, but somewhat poorer results for individual countries.

Based on the interim map, it is estimated that approximately 0.1 % of both the considered European and the EU-27 population has been exposed to concentrations above the EU annual limit value (ALV) of 40 μg/m^3. Around 64 % of both the considered European and the EU-27 population has been exposed to concentrations exceeding 10 μg/m^3 (being the WHO AQG level). The population-weighted concentration of the NO_2 annual average for 2023 for both the considered European and the EU-27 population is estimated to be about 13 μg/m^3.

Table 4.1: Population exposure and population-weighted concentration, NO_2 annual average, 2023, based on interim map

Area	Population [inhbs·1000]	NO_2 – annual average, exposed population, 2023 [%]						NO_2 ann. avg.
		< 10 μg/m^3	10-20 μg/m^3	20-30 μg/m^3	30-40 μg/m^3	40-45 μg/m^3	> 45 μg/m^3	Pop. weighted [μg/m^3/inhbs]
Northern Europe	34 055	81.1	18.1	0.7				6.8
Western Europe	86 258	42.1	48.8	7.5	1.5	0.1		11.8
Central Europe	167 045	33.4	59.8	6.4	0.4			12.4
Southern Europe	142 486	27.7	49.0	19.2	3.8	0.1	0.2	15.1
South-eastern Europe	46 106	27.2	55.0	16.2	1.5	0.1		14.3
Total	**475 951**	**35.9**	**51.2**	**11.0**	**1.7**	**0.0**	**0.1**	**12.9**
EU-27	**444 258**	**35.8**	**51.1**	**11.2**	**1.8**	**0.1**	**0.1**	**12.9**

Note: Empty cells mean no population in exposure.

Figure 4.1 shows, for the whole considered area, the population frequency distribution for exposure classes with a width of 1 μg/m^3. One can see the highest population frequency for classes between 6 and 17 μg/m^3, continuous decline of population frequency for classes between 18 and 25 μg/m^3 and continuous mild decline of population frequency for classes between 25 and 45 μg/m^3.

Figure 4.1: Population frequency distribution, NO_2 annual average 2023, based on the interim map. The WHO guideline level (10 µg/m³) is marked by the green line, the revised EU annual LV_{2030} (20 µg/m³) is marked by the yellow line, and the EU annual LV (40 µg/m³) is marked by the red line.

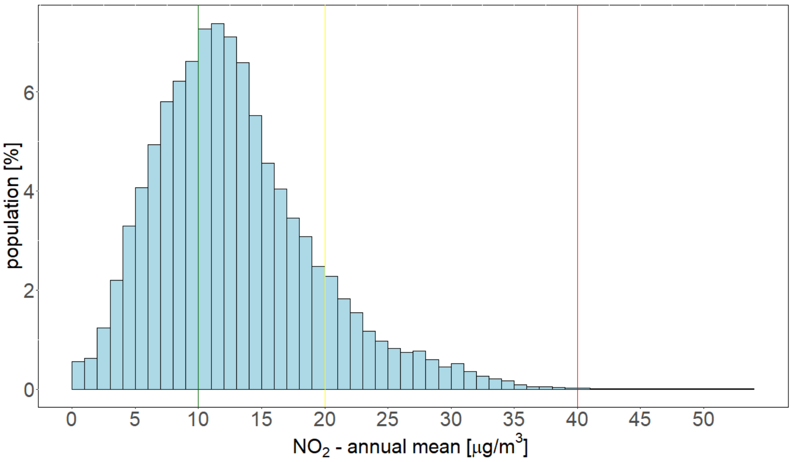

For changes in the population-weighted concentration of the NO_2 annual average in the period 2005-2023, see Figure 4.2. For the previous years, mapping results as presented in Horálek et al. (2024b and references therein) have been used. As the regular maps are not available for all years, an alternative mapping results prepared based on a subset of stations for the purpose of trend analysis 2005-2019 (Horálek et al., 2022) are also presented, in addition. Again, the population-weighted concentration for the whole area including the United Kingdom is presented for the whole period including 2023, for consistency reasons. The NO_2 concentration (in terms of annual average) shows a decrease of about 0.6 µg/m³ per year. One can see that the interim results for 2023 show the lowest estimates in the presented period.

Figure 4.2: Population-weighted concentration of NO_2 annual average in 2005-2023, based on both the regular (red) and the trend analysis (blue) mapping results (where available), and with interim results for the year 2023

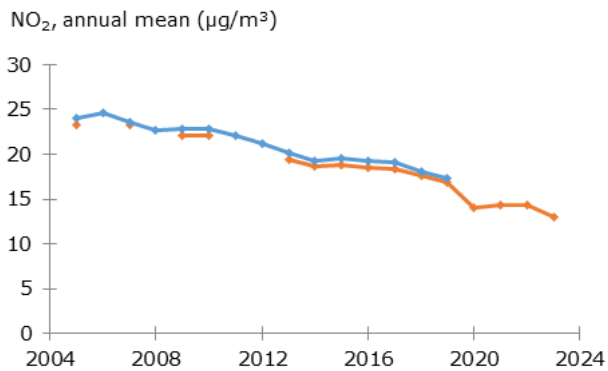

5 Conclusions

The report presents the interim 2023 maps for PM_{10} annual average, $PM_{2.5}$ annual average, NO_2 annual average and the O_3 indicator peak season average of maximum daily 8-hour means. The maps have been produced based on the non-validated E2a (UTD) data of the AQ e-reporting database, the CAMS Ensemble Forecast modelling data and other supplementary data. Together with the concentration maps, the difference maps between five-year mean 2018-2022 and 2023 and between the years 2022 and 2023 are presented (using the 2018-2022 regular and the 2023 interim maps), as well as basic exposure estimates based on the interim maps.

Regarding PM_{10} annual average, the map indicates that concentrations above the annual limit value (LV) occur mainly in urban areas of Balkan cities, including Bosnia and Herzegovina, North Macedonia, and Serbia. Additionally, elevated PM_{10} levels (30-40 µg/m^3) are estimated in parts of the Po Valley in Italy and other scattered areas in south and south-eastern Europe, while most of western and northern Europe shows concentrations below 20 µg/m^3.

$PM_{2.5}$ concentrations above the annual limit value (LV) are shown in scattered urban areas of Bosnia and Herzegovina, North Macedonia, and Serbia, while the concentrations above the indicative LV occur in the Po Valley, parts of Poland and scattered areas of central and south-eastern Europe and Greece. Most of central, southern, and south-eastern Europe has concentrations ranging from 5 to 15 µg/m^3, with northern Europe showing concentrations predominantly below 5 µg/m^3.

In the case of O_3, the map shows that in 2023 areas with a peak season (defined as the six consecutive months of the year with the highest six-month running-average O_3 concentration) average of maximum daily 8-hour means exceeding 60 µg/m^3 cover almost the entire considered region. Lower values (< 90 µg/m^3) are observed in northern Europe (Sweden, Finland, the Baltic states, Iceland), as well as in Ireland, northern Poland, Germany, the Benelux countries, in a large area of France, and in many urban areas of south-eastern Europe. Higher values (> 100 µg/m^3) are recorded in northern Italy, central Spain, and various parts of the Balkan states and Cyprus.

In the case of NO_2, no areas exceeded the annual limit value (ALV) of 40 µg/m^3 for NO_2, based on the 1 km resolution final map (although concentrations above the ALV occurred at some urban traffic locations, which are smoothed in this final map resolution). However, cities like Athens, Bucharest, Madrid, Milan, Paris, and Rome show levels above 30 µg/m^3, while major urban areas such as Belgrade, Budapest, Naples, Sofia, and Warsaw show concentrations between 20 and 30 µg/m^3. Most of Europe has NO_2 levels below 10 µg/m^3, with the Po Valley showing concentrations between 10 and 20 µg/m^3.

Uncertainty estimates based on the cross-validation of the E2a data have been performed for all interim maps, showing quite satisfactory results in general. However, these uncertainty estimates are based on the non-validated E2a data and are valid for areas covered by the E2a measurements only. The complete validation of the interim maps should be done when the validated E1a data for 2023 are available.

In the report, population exposure for only large European regions, EU-27 and the total considered area has been presented. The more detailed exposure estimates for particular European countries will be presented in 2025, in the ETC HE regular mapping report on the 2023 air quality maps created based on the validated data E1a.

List of abbreviations

Abbreviation	Name	Reference
ALV	Annual Limit Value	
AQ	Air Quality	
AQG	Air Quality Guideline of the WHO	
CLC	CORINE Land Cover	https://land.copernicus.eu/pan-european/corine-land-cover
CORINE	Co-ORdinated INformation on the Environment	https://land.copernicus.eu/pan-european/corine-land-cover
CTM	Chemical Transport model	
ECMWF	European Centre for Medium-Range Weather Forecasts	https://www.ecmwf.int/
EBAS	EMEP dataBASe	https://ebas.nilu.no/
EEA	European Environment Agency	www.eea.europa.eu
EMEP	European Monitoring and Evaluation Programme	https://www.emep.int/
ETC HE	European Topic Centre on Human health and the Environment	https://www.eionet.europa.eu/etcs
EU	European Union	https://european-union.europa.eu
GMTED	Global multi-resolution terrain elevation data	
GRIP	Global Roads Inventory Dataset	
ILV	Indicative Limit Value	
JRC	Joint Research Centre	https://ec.europa.eu/info/departments/joint-research-centre_en
LV	Limit Value	http://eur-lex.europa.eu/LexUriServ/LexUriServ.do?uri=OJ:L:2008:152:0001:0044:EN:PDF
NILU	Norwegian Institute for Air Research	https://www.nilu.no/
NO_2	Nitrogen dioxide	
O_3	Ozone	
ORNL	Oak Ridge National Laboratory	https://www.ornl.gov/
PM_{10}	Particulate Matter with a diameter of 10 micrometres or less	
$PM_{2.5}$	Particulate Matter with a diameter of 2.5 micrometres or less	
R^2	Coefficient of determination	
RIMM	Regression – Interpolation – Merging Mapping	
RMSE	Root Mean Square Error	
SOMO35	Sum of O_3 Maximum daily 8-hour means Over 35 ppb (i.e. 70 µg/m^3)	
UTC	Coordinated Universal Time	
WHO	World Health Organization	https://www.who.int/

References

CAMS, 2024, *CAMS European air quality forecasts, ENSEMBLE data. Copernicus Atmosphere Monitoring Service (CAMS) Atmosphere Data Store (ADS)* (https://ads.atmosphere.copernicus.eu/datasets/cams-europe-air-quality-forecasts?tab=overview) accessed on 21 October 2024.

Cressie, N., 1993, *Statistics for spatial data,* Wiley series, New York.

Danielson, J. J. and Gesch, D. B., 2011, *Global multi-resolution terrain elevation data 2010 (GMTED2010)*, U.S. Geological Survey Open-File Report, pp. 2011-1073 (https://pubs.er.usgs.gov/publication/ofr20111073) accessed 19 November 2020.

Defra, 2024, *UK Air information resource, Data archive*, UK Department for Environment Food & Rural Affairs (https://uk-air.defra.gov.uk/data/). Data extracted in April 2024.

EC, 2008, Directive 2008/50/EC of the European Parliament and of the Council of 21 May 2008 on ambient air quality and cleaner air for Europe, OJ L 152, 11.06.2008, 1-44 (http://eur-lex.europa.eu/LexUriServ/LexUriServ.do?uri=OJ:L:2008:152:0001:0044:EN:PDF) accessed 26 May 2021.

ECMWF, 2024, CAMS Regional: European air quality analysis and forecast data documentation. WWW: (https://confluence.ecmwf.int/display/CKB/CAMS+Regional%3A+European+air+quality+analysis+and+forecast+data+documentation) accessed 1 October 2024.

EEA, 2023, *Air Quality e-Reporting. Air quality database* (https://www.eea.europa.eu/data-and-maps/data/aqereporting-8). Data extracted in March 2023.

EEA, 2024, *Air Quality e-Reporting. Air quality database* (https://www.eea.europa.eu/data-and-maps/data/aqereporting-8). Data extracted in March 2024.

EU, 2020, *Corine land cover 2018 (CLC2018) raster data*, 100x100m^2 gridded version 2020_20 (https://land.copernicus.eu/pan-european/corine-land-cover/clc2018) accessed 19 November 2020.

Eurostat, 2020, *JRC-GEOSTAT 2018 grid dataset*, Population distribution dataset (https://ec.europa.eu/eurostat/web/gisco/geodata/reference-data/population-distribution-demography/geostat) accessed 12 April 2024.

Gilbert, R. O., 1987, *Statistical Methods for Environmental Pollution Monitoring*, Van Nostrand Reinhold, New York.

Horálek, J., et al., 2021a, *Potential use of CAMS modelling results in air quality mapping under ETC/ATNI*, Eionet Report ETC/ATNI 2019/17 (https://doi.org/10.5281/zenodo.4627762) accessed 15 June 2021.

Horálek, J., et al., 2021b, *European air quality interim mapping under ETC/ATNI*, Eionet Report ETC/ATNI 2020/11 (https://doi.org/10.5281/zenodo.5564555) accessed 12 October 2021.

Horálek, J., et al., 2022, *Air quality evolution and trends in Europe in 2005-2019 based on spatial maps,* Eionet Report ETC/ATNI 2021/11 (https://doi.org/10.5281/zenodo.6586861) accessed 15 October 2024.

Horálek, J., et al., 2023a, *Interim European air quality maps for 2021*, Eionet Report – ETC HE 2022/4 (https://doi.org/10.5281/zenodo7565623) accessed 14 September 2023.

Horálek, J., et al., 2023b, *Interim European air quality maps for 2022*, Eionet Report – ETC HE 2023/4 (https://doi.org/10.5281/zenodo7565623) accessed 1 October 2024.

Horálek, J., et al., 2024a, *Air quality maps of EEA member and cooperating countries for 2021*, Eionet Report ETC HE 2023/3 (https://doi.org/10.5281/zenodo.10589987) accessed 17 September 2024.

Horálek, J., et al., 2024b, *Air quality maps of EEA member and cooperating countries for 2022*, Eionet Report ETC HE 2024/4, *in preparation*.

JRC, 2023, *GHS-POP R2023A - GHS population grid multitemporal (1975-2030)* (https://doi.org/10.2905/2FF68A52-5B5B-4A22-8F40-C41DA8332CFE) accessed 12 April 2024.

Kuenen, J., et al., 2024, *Copernicus Atmosphere Monitoring Service regional emissions* (CAMS-REG-ANT) Copernicus Atmosphere Monitoring Service [publisher] ECCAD [distributor], (https://doi.org/10.24380/0vzb-a387) accessed 21 October 2024.

Meijer, J. R., et al., 2018, 'Global patterns of current and future road infrastructure', *Environmental Research Letters* 13, 0640 (https://doi.org/10.1088/1748-9326/aabd42) accessed 10 June 2019.

NILU, 2024, *EBAS, database of atmospheric chemical composition and physical properties* (http://ebas.nilu.no). Data extracted in April 2024.

van Geffen, J., et al., 2020, 'S5P TROPOMI NO_2 slant column retrieval: Method, stability, uncertainties and comparisons with OMI', *Atmospheric Measurement Techniques* 13, pp. 1315–1335 (https://doi.org/10.5194/amt-13-1315-2020) accessed 30 August 2021.

Veefkind, J. P., et al., 2012. 'TROPOMI on the ESA Sentinel-5 Precursor: A GMES mission for global observations of the atmospheric composition for climate, air quality and ozone layer applications', *Remote Sensing of Environment* 120, pp. 70–83 (https://doi.org/10.1016/j.rse.2011.09.027) accessed 30 August 2021.

WHO, 2021, WHO global air quality guidelines: particulate matter ($PM_{2.5}$ and PM_{10}), ozone, nitrogen dioxide, sulfur dioxide and carbon monoxide, World Health Organization (https://www.who.int/publications/i/item/9789240034228) accessed 15 October 2024.

Annex 1 Methodology

A1.1 Spatial mapping methodology

The mapping methodology used in the Regression – Interpolation – Merging Mapping method (RIMM) as routinely used in the spatial mapping under the ETC HE and its predecessors (Horálek et. al., 2024b) consists of a linear regression model followed by kriging of the residuals from that regression model (residual kriging):

$$\hat{Z}(s_0) = c + a_1 X_1(s_0) + a_2 X_2(s_0) + \cdots + a_n X_n(s_0) + \hat{\eta}(s_0) \qquad \text{(A1.1)}$$

where $\hat{Z}(s_0)$ is the estimated concentration at a point s_o,
$\hat{Z}(s_0) X_1(s_0)$ is the chemical transport model (CTM) data at point s_o,
$X_2(s_0), \ldots, X_n(s_0)$ are n-1 other supplementary variables at point s_o,
$c, a_1, a_2, \ldots, a_n$ are the n+1 parameters of the linear regression model calculated based on the data at the points of measurement,
$\hat{\eta}(s_0)$ is the spatial interpolation of the residuals of the linear regression model at point s_o, based on the residuals at the points of measurement.

For different pollutants and area types (rural, urban background, and for PM_{10}, $PM_{2.5}$ and NO_2 also urban traffic), different supplementary data are used, see Annex 1. The spatial interpolation of the regression residuals is carried out using ordinary kriging, according to

$$\hat{\eta}(s_0) = \sum_{i=1}^{N} \lambda_i \eta(s_i) \qquad \text{with } \sum_{i=1}^{N} \lambda_i = 1, \qquad \text{(A1.2)}$$

where $\hat{\eta}(s_0)$ is the interpolated value at a point s_o,
N is the number of the measurement points used in the interpolation, which is fixed based on the variogram; in any case, $20 \leq N \leq 50$,
$\eta(s_i)$ is the residual of the linear regression model at the measurement point s_i,
$\lambda_1, \ldots, \lambda_N$ are the estimated weights based on the variogram, see Cressie (1993).

For PM_{10} and $PM_{2.5}$, prior to linear regression and interpolation, a logarithmic transformation to measurements and chemical transport model (CTM) modelled concentrations is executed. After interpolation, a back-transformation is applied.

Separate map layers are created for rural and urban background areas on a grid at a resolution of 1 km (for PM and NO_2) and 10 km (for O_3), and for urban traffic areas at 1 km (for PM and NO_2). The rural background map layer is based on rural background stations, the urban background map layer is on urban and suburban background stations and the potential urban traffic map layer is based on urban and suburban traffic stations. Subsequently, the separate map layers are merged into one combined final map at 1 km resolution using weights at 1 km resolution, according to

$$\hat{Z}_F(s_0) = \left(1 - w_U(s_0)\right) \cdot \hat{Z}_R(s_0) + w_U(s_0) \left(\left(1 - w_T(s_0)\right) \cdot \hat{Z}_{UB}(s_0) + w_T(s_0) \cdot \hat{Z}_{UT}(s_0) \right) \qquad \text{for } PM_{10}, PM_{2.5} \text{ and } NO_2$$

$$= \left(1 - w_U(s_0)\right) \cdot \hat{Z}_R(s_0) + w_U(s_0) \cdot \hat{Z}_{UB}(s_0) \qquad \text{for } O_3 \qquad \text{(A1.3)}$$

where $\hat{Z}_F(s_0)$ is the resulting estimated concentration in a grid cell s_o for the final map,
$\hat{Z}_R(s_0)$, $\hat{Z}_{UB}(s_0)$ and $\hat{Z}_{UT}(s_0)$ are the estimated concentrations in a grid cell s_o for the rural background, urban background and urban traffic map layers, respectively,
$w_U(s_0)$ is the weight representing the ratio of the urban character of the grid cell s_o,
$w_T(s_0)$ is the weight representing the ratio of areas exposed to traffics in a grid cell s_o.

The weight $w_U(s_0)$ is based on the population density, while the weight $w_T(s_0)$ is based on the buffers around the roads. For details of the methodology, see Horálek et al. (2024b and references therein). In all calculations and map presentations, the EEA standard projection ETRS89-LAEA5210 is used. The mapping domain covers the whole Europe apart from Belarus, Moldova, Ukraine and the European parts of Russia, Türkiye and Kazakhstan. The presented area covers the EEA member and cooperating countries and the microstates Andorra, Monaco and San Marino. In addition, the United Kingdom is included in the population-weighted concentration calculations; in this way it is possible to show the population-weighted concentration evolution in the 19-year period 2005-2023. (Apart from graphs showing this 19-year time series, the population-weighted concentration is presented without the inclusion of the United Kingdom.)

A1.2 Pseudo station data estimation

In order to supplement the E2a measurement data, which are affected by some spatial gaps, in the mapping procedure of PM (PM_{10} and $PM_{2.5}$) and NO_2 maps we also use data from so-called *pseudo stations.* These data are concentration estimates at the locations of stations with no E2a data for the actual year Y, but with the validated E1a data for the year Y-1. As tested in Horálek et al. (2021b), these estimates are based on the relation between E2a data from year Y and validated E1a data from year Y-1, and also the ratio of the modelling or satellite data in years Y and Y-1 is used. The estimates are calculated based on the equation

$$\hat{Z}_Y(s) = c + a_1 . Z_{Y-1}(s) + a_2 . \frac{M_Y}{M_{Y-1}} . Z_{Y-1}(s) \qquad \text{(A1.4)}$$

where $\hat{Z}_Y(s)$ is the estimated concentration value at a station *s* for the year *Y*,
$Z_{Y-1}(s)$ is the measurement value at a station *s* for the year *Y-1,* based on the E1a data,
$M_Y(s)$, $M_{Y-1}(s)$ are the modelling or the satellite data at a station *s* for the years *Y* and *Y-1*,
c, a_1, a_2 are the parameters of the linear regression model calculated based on the data at the points of all stations with measurements for both Y and Y-1 years.

In the case of $PM_{2.5}$, next to the above mentioned pseudo stations, other pseudo $PM_{2.5}$ stations are also used in the locations of PM_{10} stations with no $PM_{2.5}$ measurement, similarly as in the regular mapping (Horálek et al., 2024b). These estimates are based on PM_{10} measurement E2a data for the actual year Y and different supplementary data, using linear regression:

$$\hat{Z}_{PM_{2.5}}(s) = c + b . Z_{PM_{10}}(s) + a_1 X_1(s) + a_2 X_2(s) + \cdots + a_n X_n(s) \qquad \text{(A1.5)}$$

where $\hat{Z}_{PM_{2.5}}(s)$ is the estimated value of $PM_{2.5}$ at the station *s*,
$Z_{PM_{10}}(s)$ is the measurement E2a value of PM_{10} at the station *s*,
$c, b, a_1, \ldots, a_n$ are the parameters of the linear regression model calculated based on the data at the points of stations with both $PM_{2.5}$ and PM_{10} E2a data,
$X_1(s), \ldots, X_n(s)$ are the values of other supplementary variables at the station *s*,
n is the number of other supplementary variables used in the linear regression.

In both types of pseudo stations estimates (i.e. based on both Eq. A1.4 and A1.5), all background stations (either classified as rural, urban or suburban) are handled together for estimating values at background pseudo stations, while all traffic stations used are applied for estimating values at traffic pseudo stations.

A1.3 Uncertainty analysis

The uncertainty estimation of the interim maps is based on *leave-one-out cross-validation* using the E2a data for the mapped year. This cross-validation computes the spatial interpolation for each point of measurement from all available information except from the point in question (i.e. it withholds data of one point and then makes a prediction at the spatial location of that point). This procedure is repeated for all points of measurement in the available set. The predicted and measured E2a values at these points are compared using statistical indicators and scatter plots. The main indicators used are root mean square error (RMSE), relative root mean square error (RRMSE) and bias (mean prediction error, MPE):

$$RMSE = \sqrt{\frac{1}{N}\sum_{i=1}^{N}\left(\hat{Z}(s_i) - Z(s_i)\right)^2} \qquad \text{(A1.6)}$$

$$RRMSE = \frac{RMSE}{\bar{Z}}.100 \qquad \text{(A.7)}$$

$$bias(MPE) = \frac{1}{N}\sum_{i=1}^{N}\left(\hat{Z}(s_i) - Z(s_i)\right) \qquad \text{(A1.8)}$$

where $Z(s_i)$ is the air quality measured indicator value at the i^{th} point, $i = 1, \ldots, N$,
$\hat{Z}(s_i)$ is the air quality estimated indicator value at the i^{th} point using other information, without the indicator value derived from the measured value at the i^{th} point,
$\bar{Z}$ is the mean of the values $Z(s_1), \ldots, Z(s_N)$, as measured at points $i = 1, \ldots, N$,
N is the number of the measuring points.

Other indicators are R^2 and the regression equation parameters *slope* and *intercept*, following from the scatter plot between the predicted (using cross-validation) and the observed concentrations.

RMSE and RRMSE should be as small as possible, bias (MPE) should be as close to zero as possible, R^2 should be as close to one as possible, slope a should be as close to one as possible, and intercept c should be as close to zero as possible (in the regression equation $y = a.x + c$).

It should be mentioned that the uncertainty estimates are valid only for areas covered by the E2a measurements. The complete validation of the interim maps, including the areas not covered by the E2a data, might be done when the validated E1a data are available.

A1.4 Validation

Where available, we perform the validation of both the pseudo station estimates and the concentration maps based on the validated E1a data. In this report, we perform the validation of the interim maps for 2022 (Horálek et al., 2023b). For 2023 maps, the validated E1a data are not available yet in the time designated for this report.

The validation of the pseudo station estimates is done based on the E1a measurement $PM_{2.5}$ data, where available. The statistical indicators for the validation are *standard error* and R^2.

The validation of the concentration maps is also done based on the E1a measurement $PM_{2.5}$ data. For stations with E1a $PM_{2.5}$ data and no E2a $PM_{2.5}$ data, the simple *point observation – grid prediction validation* is performed, which compares the measurement data at stations and gridded prediction values of the relevant RIMM map.

For stations with both E2a and E1a data available, the evaluation is done primarily using the *leave-one-out cross-validation*: it computes the spatial interpolation for each measurement point from all available information except from the point in question. This procedure is repeated for all measurement points in the available set. The predicted and measurement E1a values at these points are compared using statistical indicators and a scatter plot. Additionally, the simple point observation – grid prediction validation is also performed for these stations.

The results of both cross-validation and simple validation are described by the statistical indicators and scatter plots. The main indicators used are RMSE, RRMSE and bias (see Eq. A1.6-A1.8). Other indicators are R^2 and the regression equation parameters, following from the scatter plot between the predicted (using either cross-validation or simple validation) and the observed concentrations.

A1.5 Population exposure calculation and estimation of trends

Population exposure and population-weighted concentration for large regions, for EU-27 and for the whole presented area are calculated based on the air quality maps (and map layers) and population density data, as described in Horálek et al. (2024b). For detecting and estimating the trends in time series of annual values of population exposure, the non-parametric Mann-Kendall's test for detecting the presence of the monotonic trend and the non-parametric Sen's method for estimating the slope of a linear trend are executed, see Gilbert (1987).

A1.6 Geographical division of the considered European area used in the assessment

The tables of population exposure and population-weighted concentration present the country grouping of the following large regions: 1) Northern Europe (N): Denmark (including Faroes), Estonia, Finland, Iceland, Latvia, Lithuania, Norway, Sweden; 2) Western Europe (W): Belgium, France north of 45°, Ireland, Luxembourg, Netherlands; 3) Central Europe (C): Austria, Czechia, Germany, Hungary, Liechtenstein, Poland, Slovakia, Slovenia, Switzerland; 4) Southern Europe (S): Andorra, Cyprus, France south of 45°, Greece, Italy, Malta, Monaco, Portugal, San Marino, Spain; 5) South-eastern Europe (SE): Albania, Bosnia and Herzegovina, Bulgaria, Croatia, Montenegro, North Macedonia, Romania, Serbia, and Kosovo. Note that the designation of the large regions is intended primarily for the assessments of the mapping reports and does not necessarily follow common geographic or geopolitical terms.

Annex 2 Data used

A2.1 Air quality monitoring data

For the interim maps, we have used air quality station 2023 monitoring data coming from the E2a data set of the Air Quality e-Reporting database (EEA, 2024). The data of the up-to-date (UTD) dataflow E2a are being provided on an hourly basis from most of the EEA's member and cooperating countries. This data set has been supplemented with United Kingdom stations ([2]) from the Defra database (Defra, 2024).

For the purposes of the pseudo stations' calculations and validation, the 2022 data of the E1a data set of the Air Quality e-Reporting database (EEA, 2024) have been used. The data of the dataflow E1a is submitted to the EEA by the reporting countries every September and covers the year before the delivery. This E1a data set has been supplemented with several EMEP rural stations from the database EBAS (NILU, 2024) not reported to the Air Quality e-Reporting database and with United Kingdom stations from the Defra database (Defra, 2024).

The following pollutants and aggregations are considered:

PM_{10} – annual average [μg/m^3], years 2022 (E1a) and 2023 (E2a),
$PM_{2.5}$ – annual average [μg/m^3], years 2022 (E1a) and 2023 (E2a),
O_3 – peak season average of maximum daily 8-hour means [μg/m^3], year 2023 (E2a),
NO_2 – annual average [μg/m^3], years 2022 (E1a) and 2023 (E2a).

For PM_{10}, $PM_{2,5}$ and NO_2 we use the stations classified as background (for all the three types of area, i.e. rural, suburban and urban), and also traffic for the types of area suburban and urban. For O_3, we use only data from stations classified as background (for the three types of area). In the mapping, rural background stations are used for the rural map layer, urban and suburban stations for the urban background map layer and urban and suburban traffic stations for the urban traffic map layer (Section A1.1). Industrial stations are not used, as their local concentration levels cannot be easily generalized for the whole map. Only stations with an annual data coverage of at least 75 percent are used.

Table A2.1 shows the number of stations used in the 2023 interim mapping of PM_{10} and $PM_{2.5}$. In the RIMM mapping (as described in Section 2.1) of the year 2023, E2a 2023 stations are used, together with pseudo stations derived from E1a stations of the year 2022. The pseudo stations are located at the places of the E1a 2022 stations with no (or not sufficient) E2a data for the year 2023 (labelled "For pseudo 2023"). The rest of the E1a 2022 stations (with both E1a data for 2022 and E2a data for 2023, labelled "For regression") are used for estimation of the parameters of the linear regression for the pseudo stations calculation (see Eq. A1.4).

([2]) The United Kingdom exited the European Union in January 2020 and does not report the air quality data to the AQ e-reporting database. Nevertheless, in order to enable the interpolation across the whole mapping domain, the publicly available data from the Defra database have been also used in the analysis.

Table A2.1: Number of stations used in interim mapping 2023 per station type, for PM_{10} (left) and NO_2 (right)

Station type	PM_{10}				$PM_{2.5}$			
	E1a 2022			E2a 2023	E1a 2022			E2a 2023
	Total	For regression	For pseudo 2023	Mapping 2023	Total	For regression	For pseudo 2023	Mapping 2023
Rural background	406	280	126	297	269	173	96	191
Urban/suburb. backgr.	1161	1107	524	1176	995	707	288	774
Urban/suburb. traffic	808	626	182	669	465	374	91	408

For the $PM_{2.5}$ mapping, in addition to the $PM_{2.5}$ stations, 104 rural background, 117 urban/suburban background and 275 urban/suburban traffic PM_{10} E2a 2023 stations (at locations without $PM_{2.5}$ measurement either for 2023 or 2022) have been also used for the purpose of calculating the pseudo $PM_{2.5}$ station data (see Eq. A1.5).

Table A2.2 shows the number of stations used in the interim mapping of O_3 and NO_2. In the O_3 interim mapping, only E2a 2023 stations are used. No pseudo stations for O_3 are used due to quite complete spatial coverage of the E2a O_3 data.

Table A2.2: Number of stations used in interim mapping 2023 per station type, for O_3 and NO_2

Station type	O_3	NO_2			
	E2a 2023	E1a 2022			E2a 2023
	Mapping 2023	Total	For regression	For pseudo 2023	Mapping 2023
Rural background	463	506	390	116	399
Urban/suburb. backgr.	965	1487	1192	295	1238
Urban/suburb. traffic	–	1286	919	367	958

A2.2 Chemical transport modelling (CTM) data

The CAMS Ensemble Forecast data as provided by the Copernicus Atmosphere Monitoring Service (CAMS) at a regional scale over Europe have been used. The European regional production consists of an ensemble of eleven air quality models run operationally. All models use the same CAMS-REG anthropogenic emissions and current meteorology from the operational ECMWF IFS forecast. The models provide (along with other products) a 96-hour forecast made available at 08:00 UTC the day of the forecast. The forecast data product is available on an hourly time resolution and at a spatial resolution of 0.1° x 0.1°, which corresponds roughly to 5-10 km (W–E) x 10 km (S–N). Each model forecast is combined into an ensemble forecast by taking the median of all used models. For further details see ECMWF (2024).

In this report, the CAMS Ensemble Forecast data (for the lead hour 0-23) for 2022 and 2023 have been used (CAMS, 2024). All the models used in the ensemble were run using the CAMS-REG-v5.1 REF2 v2.0.1 emissions (corresponding to year 2018) for most of the years 2022 and 2023 (implemented in March), while before March 2022, CAMS-REG-AP_v4.2_REF2.1 emissions representing year 2017, and since November 2023, CAMS-REG-v6.1 emissions representing year 2022 were used instead (ECMWF, 2024). For more information on emissions, see Kuenen et al., 2024. All modelling data have been aggregated into the annual statistics and converted into the reference EEA 1 km (for PM and NO_2) and 10 km (for O_3) grids. The pollutants and parameters used are the same as those used for the monitoring data.

A2.3 Satellite data

Data from the TROPOspheric Monitoring Instrument (TROPOMI) onboard of the Sentinel-5 Precursor satellite (Veefkind et al., 2012) was used. Their spatial resolution is approximately 5.5 km by 3.5 km. The product used is the S5P_OFFL_L2__NO2 product (van Geffen et al., 2020) and it provides the tropospheric vertical column density of nitrogen dioxide (NO_2), i.e. a vertically integrated value over the entire troposphere. All overpasses for a specific day were then mosaicked and gridded into the reference EEA 1 km grid in the ETRS89 / ETRS-LAEA (EPSG 3035) projection. The daily gridded files have been subsequently averaged to an annual mean. The annual mean has been aggregated from cloud-free high-quality (qa_value > 0.75) daily data only. The parameter used is

NO_2 – annual average tropospheric vertical column density (VCD) [number of NO_2 molecules per cm^2 of earth surface], years 2022 and 2023.

A2.4 Other supplementary data

Meteorological data

The meteorological data used are the ECWMF data extracted from the CDS (Climate Data Store, https://cds.climate.copernicus.eu/cdsapp#!/home). Specifically, the hourly data of the reanalysed data set ERA5-Land in 0.1°x0.1° resolution have been used. In the coastal areas (where the data from ERA5-Land are not available), the same parameters from the reanalysed data set ERA5 in 0.25°x0.25° resolution have been applied. The hourly data have been derived into the parameters needed, aggregated into the annual statistics and converted into the reference EEA 1 km (for PM and NO_2) and 10 km (for O_3) grids. For details, see Horálek et al. (2024b). Meteorological parameters used are *wind speed* (annual mean for 2023, in $m.s^{-1}$), *surface net solar radiation* (annual mean of daily sum for 2023, in $MWs.m^{-2}$) and *relative humidity* (annual mean for 2023, in percentage).

Altitude

The altitude data field (in m) of Global Multi-resolution Terrain Elevation Data 2010 (GMTED2010) has been used, with an original grid resolution of 15 arcseconds coming from U.S. Geological Survey Earth Resources Observation and Science, see Danielson and Gesch (2011). The data were converted into the EEA reference grids in 1 km and 10 km resolutions. Next to this, another aggregation based on the 1 km grid cells has been executed, i.e. the average of the circle with a radius of 5 km, calculated as a floating average for all 1 km grid cells.

Land cover

CORINE Land Cover 2018 – grid 100 m, Version 2020_20 (EU, 2020) is used. The 44 CLC classes have been re-grouped into the 8 more general classes. In this paper, we use five of these general classes, namely high density residential areas (HDR), low density residential areas (LDR), agricultural areas (AGR), natural areas (NAT), and traffic areas (TRAF). For details, see Horálek et al. (2024b). Two aggregations are used, i.e., into 1 km grid and into the circle with radius of 5 km. The aggregated grid value represents for each general class the total area of this class as percentage of the total area of the 1 km x 1 km square or the circle with radius of 5 km.

Population density and Road data

Population density (in inhabitants/km^2) is based on JRC-Geostat 2018 grid dataset, Eurostat (2020). For regions not included in the JRC-Geostat 2018 dataset, GHS population grid for 2020 (JRC, 2023) scaled to the reference year 2018 is used. For details, see Horálek et al. (2024b). GRIP vector road type data is used (Meijer et al., 2018). Based on these data (i.e., buffers around the roads), traffic map layers (Section 2.1) are merged into the final maps (Horálek et al., 2024b).

Annex 3 Technical details and uncertainties of interim maps

This Annex 3 presents different technical details on the interim maps presented in this report. Sections A3.1, A3.2, A3.3 and A3.4 gives technical details and uncertainty estimates of the 2023 interim maps for PM_{10}, $PM_{2.5}$, O_3 and NO_2, respectively.

A3.1 Particulate matter PM_{10}

This section presents the technical details and uncertainty estimates of the PM_{10} 2023 annual average interim map as presented in Map 2.1.

Like in Horálek et al. (2021b), first, the pseudo stations data have been estimated. The estimates have been calculated based on the E1a measurement data for 2022, the CAMS Ensemble Forecast modelling data for 2022 and 2023, and the regression relation with the E2a measurement data for 2023. Table A3.1 presents the regression coefficients determined for pseudo stations data estimation, based on the 1387 rural and urban/suburban background and 626 urban/suburban traffic stations that have both E1a 2022 and E2a 2023 measurements available (see Sections A1.2 and A2.1). Next to this, it presents the statistics showing the tentative quality of the estimate.

Table A3.1: Parameters and statistics of the linear regression model for the generation of pseudo PM_{10} data in rural and urban background and urban traffic areas, for PM_{10} annual average 2023

PM_{10} – Annual average		Rural and urban background areas	Urban traffic areas
Linear regression model (LRM, Eq. 2.4)	c (constant)	1.0	1.3
	a1 (PM_{10} annual mean 2022, E1a data)	0.406	0.503
	a2 (PM_{10} annual mean 2022 * CAMS ratio 2023/2022)	0.450	0.347
	Adjusted R^2	**0.91**	**0.87**
	Standard Error [μg/m^3]	**1.7**	**2.1**

Based on the E2a data and pseudo data, CAMS Ensemble Forecast modelling data and other supplementary data as used in the regular mapping, the interim PM_{10} annual average map for 2023 has been created (see Map 2.1). Table A3.2 presents the estimated parameters of the linear regression models (c, a_1, a_2,…) and of the residual kriging (*nugget, sill, range*) and includes the statistical indicators of both the regression and the kriging of its residuals.

Table A3.2 shows that the uncertainty of the interim map of PM_{10} annual average expressed by RMSE is about 2 μg/m^3 for the rural areas and 3 μg/m^3 for both the urban background and the urban traffic areas. The relative mean uncertainty (Relative RMSE) of this map is 19 % for rural, and 18 % for both urban background and urban traffic areas. However, these uncertainty estimates are based on the non-validated E2a data and are valid only for areas covered by the E2a stations. The complete validation of the interim PM_{10} map can only be done when the validated E1a data for 2023 are available.

Table A3.2: Parameters and statistics of the linear regression model and ordinary kriging in rural, urban background and urban traffic areas for the interim map of PM_{10} annual average 2023

PM_{10}		Annual average		
		Rural areas	Urban b. areas	Urban tr. areas
Linear regression model (LRM, Eq. 2.1)	c (constant)	1.52	0.89	1.72
	a1 (log. CAMS-ENS FC model)	0.786	0.78	0.536
	a2 (altitude GMTED)	-0.00015		
	a3 (relative humidity)	-0.011		
	a4 (wind speed)	-0.037		-0.052
	a5 (land cover NAT1)	-0.0010		
	Adjusted R^2	**0.65**	**0.36**	**0.43**
	Standard Error [μg/m³]	**0.24**	**0.31**	**0.25**
Ordinary kriging (OK) of LRM residuals	nugget	0.014	0.013	0.013
	sill	0.055	0.043	0.039
	range [km]	1000	150	410
LRM + OK of its residuals	**RMSE [μg/m³]**	**2.4**	**3.1**	**3.3**
	Relative RMSE [%]	**18.6**	**18.1**	**17.5**
	Bias (MPE) [μg/m³]	**0.1**	**0.1**	**-0.1**
	R^2 of cross.-val. regr. equation	**0.74**	**0.70**	**0.69**
	Slope of cross-val. regr. equation	**0.78**	**0.75**	**0.69**
	Intercept of cross-val. regr. equation	**2.9**	**4.4**	**5.7**

A3.2 Particulate matter $PM_{2.5}$

This section presents the technical details and uncertainty estimates of the $PM_{2.5}$ 2023 annual average interim map as presented in Map 2.3.

Like in Horálek et al. (2023b), the pseudo stations data of two types have been estimated at first, i.e. based on the $PM_{2.5}$ E1a measurement data for 2022, the CAMS Ensemble Forecast modelling data for 2022 and 2023, and the regression relation with the $PM_{2.5}$ E2a measurement data for 2023 (see Eq. A1.4) and based on the PM_{10} E2a measurement data for 2023, different supplementary data, and the regression relation with the $PM_{2.5}$ E2a measurement data for 2023 (see Eq. A1.5). Table A3.3 presents the regression coefficients determined for these pseudo stations data estimations.

Table A3.3: Parameters and statistics of the linear regression model for the generation of pseudo $PM_{2.5}$ data in rural and urban background and urban traffic areas for $PM_{2.5}$ annual average 2023, using $PM_{2.5}$ E1a data for 2022 (top) and PM_{10} E2a data for 2023 (bottom)

$PM_{2.5}$ - Annual average		Rural and urban background areas	Urban traffic areas
Linear regression model (LRM, Eq. 2.4)	c (constant)	0.4	0.5
	a1 ($PM_{2.5}$ annual mean 2022, E1a measurement data)	0.645	0.840
	a2 ($PM_{2.5}$ annual mean 2022 * CAMS ratio 2023/2022)	0.214	*n.sign.*
	Adjusted R^2	**0.90**	**0.91**
	Standard Error [μg/m³]	**1.2**	**1.2**
Linear regresion model (LRM, Eq. 2.5)	c (constant)	20.8	42.0
	b (PM_{10} annual mean 2023, E2a measurement data)	0.623	0.358
	a1 (surface solar radiation 2023)	-0.0028	-0.0036
	a2 (latitude)	-0.246	-0.552
	a3 (longitude)	0.089	0.152
	Adjusted R^2	**0.83**	**0.72**
	Standard Error [μg.m⁻³]	**1.6**	**2.2**

The estimates based on the $PM_{2.5}$ E1a data for 2022 have been calculated using 880 rural and urban/suburban background and 374 urban/suburban traffic stations that have both E1a 2022 and E2a 2023 data available, while the estimates based on the PM_{10} E2a data for 2023 using 888 rural and urban/suburban background and 369 urban/suburban traffic stations that have both PM_{10} and $PM_{2.5}$ E2a 2023 data available.

Similarly as in Horálek et al. (2023b), the estimates based on the $PM_{2.5}$ data for 2022 show stronger correlation with the $PM_{2.5}$ data for 2023, compared to the estimates based on the PM_{10} data for 2023. Leading from this, the pseudo data estimates based on the PM_{10} data for 2023 have been applied only in places with no pseudo data estimates based on the $PM_{2.5}$ data for 2022. For the number of $PM_{2.5}$ data and pseudo $PM_{2.5}$ data of both types applied in the interim map creation, see Section 3.1.

Based on the E2a data and pseudo data, CAMS Ensemble Forecast modelling data and other supplementary data as used in the regular mapping, the interim $PM_{2.5}$ annual average map for 2023 has been created. Table A3.4 presents the estimated parameters of the linear regression models (*c, a_1, a_2,…*) and of the residual kriging (*nugget, sill, range*) and includes the statistical indicators of both the regression and the kriging of its residuals.

Table A3.4: Parameters and statistics of the linear regression model and ordinary kriging in rural, urban background and urban traffic areas for the interim map of $PM_{2.5}$ annual average 2023

$PM_{2.5}$ – Annual average		Rural areas	Urban b. areas	Urban tr. areas
Linear regresion model (LRM, Eq. 2.1)	c (constant)	0.76	0.61	0.72
	a1 (log. CAMS-ENS-FC model)	0.727	0.75	0.695
	a2 (altitude GMTED)	-0.00021		
	a3 (wind speed)	-0.059		
	a4 (land cover NAT1)	*-0.0011*		
	Adjusted R^2	**0.64**	**0.46**	**0.56**
	Standard Error [μg/m³]	**0.24**	**0.27**	**0.26**
Ordinary kriging (OK) of LRM	nugget	0.033	0.020	0.140
	sill	0.052	0.055	0.162
	range [km]	1000	200	320
LRM + OK of its residuals	**RMSE [μg/m³]**	**1.4**	**2.2**	**2.1**
	Relative RMSE [%]	**18.7**	**21.3**	**20.2**
	Bias (MPE) [μg/m³]	**0.2**	**0.1**	**0.0**
	R^2 of cross.-val. regr. equation	**0.79**	**0.71**	**0.76**
	Slope of cross-val. regr. equation	**0.73**	**0.74**	**0.73**
	Intercept of cross-val. regr. equation	**2.2**	**2.7**	**2.7**

Table A3.4 shows that the uncertainty of the interim map of $PM_{2.5}$ annual average expressed by RMSE is about 1 μg/m³ for the rural areas and 2 μg/m³ for both the urban background and the urban traffic areas. The relative mean uncertainty (Relative RMSE) of this map is 19 % for rural areas, 21 % for the urban background areas and 20 % for the urban traffic areas. However, these uncertainty estimates are based on the non-validated E2a data and are valid only for areas covered by the E2a stations. The complete validation of the interim $PM_{2.5}$ map can only be done when the validated E1a data for 2023 are available.

A3.3 Ozone

Similarly as in Horálek et al. (2023b), no pseudo stations for O_3 have been used, due to a quite complete spatial coverage of the E2a data. Based on the E2a data, CAMS Ensemble Forecast modelling data and other supplementary data as used in the regular mapping, the interim map of the O_3 indicator peak season average of maximum daily 8-hour means for 2023 has been created (see Map 3.1). Table A3.5 presents the estimated parameters of the linear regression models (*c, a_1, a_2,…*) and of the residual kriging (*nugget, sill, range*) and includes the statistical indicators of the regression and the kriging of its residuals.

Table A3.5: Parameters and statistics of the linear regression model and ordinary kriging in rural and urban background areas for the interim map of O_3 indicator peak season average of maximum daily 8-hour means for 2023

O_3 – Peak season average of maximum daily 8-hour means		Rural background areas	Urban background areas
Linear regresion model (LRM, Eq. 2.1)	c (constant)	5.7	33.2
	a1 (CAMS-ENS-FC model)	0.94	0.68
	a2 (altitude GMTED)	0.01	
	a3 (wind speed)		-1.6
	a4 (s. solar radiation)	*n. sign.*	*n.sign.*
	Adjusted R^2	**0.56**	**0.35**
	Standard Error [μg/m^3·d]	**5.9**	**9**
Ord. krig. (OK) of LRM residuals	nugget	21	21
	sill	35	50
	range [km]	790	360
LRM + OK of its residuals	**RMSE [[μg/m^3·d]**	**5.6**	**7.2**
	Relative RMSE [%]	**6.0**	**8.0**
	Bias (MPE) [μg/m^3·d]	**0.0**	**0.0**
	R^2 of cross.-val. regr. equation	**0.61**	**0.56**
	Slope of cross-val. regr. equation	**0.61**	**0.59**
	Intercept of cross-val. regr. equation	**35.7**	**37.0**

Table A3.5 shows that the uncertainty of the interim map of O_3 indicator peak season average of maximum daily 8-hour means expressed by RMSE is 36 μg/m^3 for the rural areas and 37 μg/m^3 for the urban background areas. These uncertainty estimates are based on the non-validated E2a data and are valid only for areas covered by the E2a stations. The complete validation of the interim O_3 map can only be done when the validated E1a data for 2023 are available.

A3.4 Nitrogen dioxide

As a first step for the interim NO_2 annual average 2023 map creation, the pseudo stations data have been estimated, based on the E1a measurement data for 2022, the Sentinel-5P satellite data for 2022 and 2023, and the regression relation with the E2a measurement 2023 data. Table A3.6 presents the regression coefficients determined for pseudo stations data estimation, based on the 1582 rural and urban/suburban background and 919 urban/suburban traffic stations that have both E1a 2022 and E2a 2023 measurements available (see Sections A1.2 and A2.1). Apart from this, it gives the statistics showing the tentative quality of the estimate.

Table A3.6: Parameters and statistics of the linear regression model for generation of pseudo NO_2 data in rural and urban background and urban traffic areas, for NO_2 annual average 2023

NO_2 – Annual average		Rural and urban background areas	Urban traffic areas
Linear regression model (LRM, Eq. 2.4)	c (constant)	0.0	0.1
	a1 (NO_2 annual mean 2022, E1a data)	0.712	0.832
	a2 (NO_2 annual mean 2022 * Sentinel-5P ratio 2023/2022)	0.211	0.107
	Adjusted R^2	**0.94**	**0.92**
	Standard Error [μg/m³]	**1.5**	**2.2**

Based on the E2a data and pseudo data, CAMS Ensemble Forecast modelling data, Sentinel-5P satellite data and other supplementary data as used in the regular mapping, the interim NO_2 annual average map for 2023 has been created (see Map 4.1). Table A3.7 presents the estimated parameters of the linear regression models (*c, a_1, a_2,…*) and of the residual kriging (*nugget, sill, range*) and includes the statistical indicators of both the regression and the kriging of its residuals.

Table A3.7: Parameters and statistics of the linear regression model and ordinary kriging in rural, urban background and urban traffic areas for the interim map of NO_2 annual average 2023

NO_2		Annual average		
		Rural areas	Urb. b. areas	Urb. tr. areas
Linear regresion model (LRM, Eq. 2.1)	c (constant)	4.9	12.1	19.31
	a1 (CAMS-ENS-FC model)	0.295	*n.sign.*	*n.sign.*
	a6 (satellite Sentinel-5P)	1.15	2.300	2.550
	a2 (altitude)	*n.sign.*		
	a3 (altitude_5km_radius)	*n.sign.*		
	a4 (wind speed)	-0.76	-2.038	-2.347
	a7 (population*1000)	0.00138	0.00029	
	a8 (NAT_1km)		-0.0360	
	a9 (AGR_1km)		-0.0177	
	a10 (TRAF_1km)		0.0682	
	a11 (LDR_5km_radius)	*n.sign.*	*n.sign.*	0.0720
	a12 (HDR_5km_radius)		0.0471	0.2057
	a13 (NAT_5km_radius)	-0.0343		
	Adjusted R^2	**0.61**	**0.50**	**0.36**
	Standard Error [μg/m³]	**2.5**	**5.0**	**7.6**
Ordinary kriging (OK) of LRM residuals	nugget	3	8	19
	sill	5	13	34
	range [km]	700	130	140
LRM + OK of its residuals	**RMSE [μg/m³]**	**1.8**	**3.5**	**5.6**
	Relative RMSE [%]	**31.3**	**25.1**	**23.7**
	Bias (MPE) [μg/m³]	**0.0**	**0.0**	**-0.2**
	R^2 of cross.-val. regr. equation	**0.75**	**0.61**	**0.50**
	Slope of cross-val. regr. equation	**0.75**	**0.66**	**0.54**
	Intercept of cross-val. regr. equation	**1.5**	**4.7**	**10.7**

Table A3.7 shows that the uncertainty of the interim map of NO_2 annual average expressed by RMSE is about 2 µg/m^3 for the rural areas, 3.5 µg/m^3 for the urban background areas, and 6 µg/m^3 for the urban traffic areas, respectively. The relative mean uncertainty (Relative RMSE) of this map is 31 % for rural areas, 25 % for urban background areas and 24 % for urban traffic areas. However, like for other pollutants, these uncertainty estimates are based on the non-validated E2a data and are valid only for areas covered by the E2a stations. The complete validation of the interim NO_2 map can only be done when the validated E1a data for 2023 are available.

Annex 4 Validation of 2022 interim maps and exposure estimates

This Annex 4 presents the validation of the 2022 interim maps produced using the up-to-date E2a data (EEA, 2023) as presented in Horálek et al. (2023b), against the validated E1a data (EEA, 2024). Next to this, it presents the exposure tables calculated using the interim 2022 maps and validates them against the exposure estimates calculated using the regular 2022 maps as presented in Horálek et al. (2024a).

A4.1 Concentration maps

This section evaluates the concentration interim maps against the E1a data, using cross-validation.

PM$_{10}$

Table A4.1 presents the evaluation of the interim PM$_{10}$ annual average 2022 map, against the E1a station data for 2022. Additionally, it also presents the cross-validation evaluation of the regular PM$_{10}$ annual average 2022 map (Horálek et al., 2024b) for the same subsets of the E1a station data, for comparable reasons.

Table A4.1: Validation of interim (left) and regular (right) map of PM$_{10}$ annual average 2022 showing RMSE, RRMSE, bias, R^2 and linear regression from validation scatter plots in rural background (top), urban background (middle) and urban traffic areas (bottom), against two validation sets of stations. Units: µg/m^3 except for RRMSE and R^2

PM$_{10}$ – Annual Average											
Area	Validation set	Interim map					Regular map				
		RMSE	RRMSE	Bias	R^2	Regr. eq.	RMSE	RRMSE	Bias	R^2	Regr. eq.
Rural	E1a stations – all	2.6	17.4%	0.1	0.766	y = 0.761x + 3.6	2.9	19.9%	0.0	0.699	y = 0.749x + 3.8
	E1a stations with no E2a data	2.6	16.1%	-0.5	0.766	y = 0.739x + 3.7	3.4	21.2%	-0.5	0.700	y = 0.754x + 3.5
Urban background	E1a stations – all	3.8	18.8%	0.0	0.643	y = 0.702x + 6.0	3.9	19.5%	0.1	0.620	y = 0.689x + 6.4
	E1a stations with no E2a data	5.3	23.6%	-0.3	0.510	y = 0.560x + 9.6	5.6	24.7%	-0.1	0.462	y = 0.518x + 10.8
Urban traffic	E1a stations – all	3.6	17.2%	0.0	0.664	y = 0.670x + 7.0	3.9	18.4%	0.0	0.628	y = 0.729x + 5.7
	E1a stations with no E2a data	4.2	17.4%	0.4	0.634	y = 0.672x + 7.7	4.4	19.7%	0.7	0.582	y = 0.743x + 6.5

One can see that the uncertainty of the interim map is the same or even slightly better compared to the uncertainty of the regular map. The reason for the slightly worse performance of the regular map probably is in the inclusion of the stations of Türkyie in the case of the regular map.

Additionally, the validation of the E2a data and the pseudo station data used in the interim PM$_{10}$ mapping has been performed. Table A4.2 shows the validation of the E2a and the pseudo data against the E1a station data in the locations of these stations.

Table A4.2: Validation of E2a and pseudo station data showing RMSE, RRMSE, bias, R^2 and linear regression from validation scatter plots for rural background (top), urban/suburban background (middle) and urban/suburban traffic stations (bottom), PM$_{10}$ annual average 2022. Validation by E1a station data. Units: µg/m^3 except for RRMSE and R^2

PM$_{10}$ – Annual Average							
Station type	Evaluated set	Validation set	RMSE	RRMSE	Bias	R^2	Regr. eq.
Rural background	E2a stations	E1a stations with E2a data	0.8	5.5%	0.1	0.975	y = 0.986x + 0.3
	Pseudo stations	E1a stations in locations of pseudo stations	1.7	10.6%	0.1	0.925	y = 0.912x + 1.5
Urban/suburban background	E2a stations	E1a stations with E2a data	0.9	4.8%	0.0	0.972	y = 0.990x + 0.2
	Pseudo stations	E1a stations in locations of pseudo stations	2.7	12.0%	0.0	0.869	y = 0.924x + 1.7
Urban/suburban traffic	E2a stations	E1a stations with E2a data	1.6	7.5%	0.0	0.937	y = 0.971x + 0.6
	Pseudo stations	E1a stations in locations of pseudo stations	3.0	12.9%	0.0	0.739	y = 0.862x + 3.2

In general, the results show better agreement of the pseudo data with the E1a data, compared to the validation of the pseudo stations presented in Horálek et al. (2021a), which recommended the use of the pseudo stations.

Map A4.1 shows the difference between the interim and the regular maps of the PM_{10} annual average 2022, for rural and urban background map layers. One can see the greatest differences in Balkan, Cyprus and Hungary, i.e. in the areas with the lack of the E1a stations.

Map A4.1: Difference between interim and regular map for PM_{10} annual average 2022 in rural (left) and urban background (right) areas. Urban map layer is applicable in urban areas only

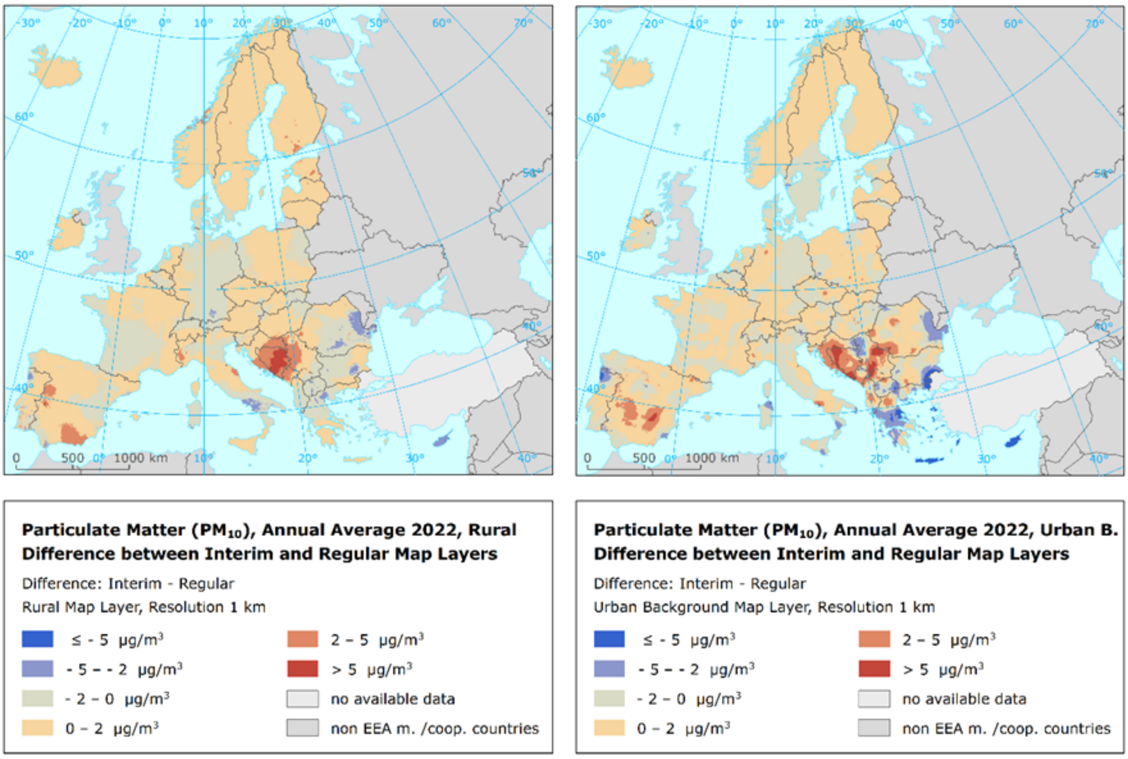

$PM_{2.5}$

Table A4.3 shows the evaluation of the interim $PM_{2.5}$ annual average 2022 map, against the E1a station data for 2022. Additionally, it also presents the cross-validation evaluation of the regular $PM_{2.5}$ annual average 2022 map (Horálek et al., 2024b) for the same subsets of the E1a station data, for comparable reasons.

Table A4.3: Validation of interim (left) and regular (right) map of $PM_{2.5}$ annual average 2022 showing RMSE, RRMSE, bias, R^2 and linear regression from validation scatter plots in rural background (top), urban background (middle) and urban traffic areas (bottom), against two validation sets of stations. Units: µg/m³ except for RRMSE and R^2

$PM_{2.5}$ – Annual Average											
	Validation set	Interim map					Regular map				
		RMSE	RRMSE	Bias	R^2	Regr. eq.	RMSE	RRMSE	Bias	R^2	Regr. eq.
Rural	E1a stations – all	2.2	24.1%	-0.1	0.713	y = 0.669x + 2.9	2.3	25.0%	0.0	0.689	y = 0.703x + 2.7
	E1a stations with no E2a data	2.3	22.5%	-0.1	0.712	y = 0.728x + 2.7	2.2	21.8%	-0.1	0.731	y = 0.784x + 2.1
Urban background	E1a stations – all	2.6	21.7%	0.0	0.683	y = 0.706x + 3.6	2.7	21.9%	0.2	0.685	y = 0.762x + 3.1
	E1a stations with no E2a data	3.4	25.1%	-0.4	0.625	y = 0.637x + 4.6	3.5	25.2%	0.1	0.626	y = 0.696x + 4.3
Urban traffic	E1a stations – all	2.2	19.1%	0.0	0.777	y = 0.796x + 2.3	2.2	19.5%	-0.1	0.767	y = 0.744x + 2.8
	E1a stations with no E2a data	2.9	20.7%	-0.3	0.795	y = 0.832x + 2.0	3.1	22.2%	-0.6	0.770	y = 0.733x + 3.1

One can see that the uncertainty of the interim map is at the similar level as the uncertainty of the regular map.

Additionally, the validation of the E2a data and the pseudo station data used in the interim $PM_{2.5}$ mapping has been performed. Table A4.4 shows the validation of the E2a and the pseudo data, against the E1a station data in the locations of these stations.

Table A4.4: Validation of E2a and pseudo station data showing RMSE, RRMSE, bias, R^2 and linear regression from validation scatter plots for rural background (top), urban/suburban background (middle) and urban/suburban traffic stations (bottom), $PM_{2.5}$ annual average 2022. Validation by E1a station data. Units: µg/m³ except for RRMSE and R^2

$PM_{2.5}$ – Annual Average							
Station type	Evaluated set	Validation set	RMSE	RRMSE	Bias	R^2	Regr. eq.
Rural background	E2a stations	E1a stations with E2a data	0.7	8.5%	0.0	0.966	y = 0.930x + 0.6
	Pseudo stations	E1a stations in locations of pseudo stations	1.2	11.9%	-0.1	0.920	y = 0.879x + 1.1
Urban/suburban background	E2a stations	E1a stations with E2a data	0.6	5.5%	0.0	0.976	y = 0.995x + 0.1
	Pseudo stations	E1a stations in locations of pseudo stations	1.9	14.0%	-0.3	0.864	y = 0.882x + 1.3
Urban/suburban traffic	E2a stations	E1a stations with E2a data	0.6	5.3%	0.0	0.976	y = 0.969x + 0.3
	Pseudo stations	E1a stations in locations of pseudo stations	3.0	20.3%	-0.2	0.816	y = 0.984x

In general, the results show better agreement of the pseudo data with the E1a data, compared to the validation of the pseudo stations used in the 2022 interim mapping (Horálek et al., 2023b).

Map A4.2 shows the difference between the interim and the regular maps of the $PM_{2.5}$ annual average 2022, for rural and urban background map layers. One can see the greatest differences in Balkan and Cyprus, i.e. in the areas with the lack of the E1a stations.

Map A4.2: Difference between interim and regular map for $PM_{2.5}$ annual average 2022 in rural (left) and urban background (right) areas. Urban map layer is applicable in urban areas only

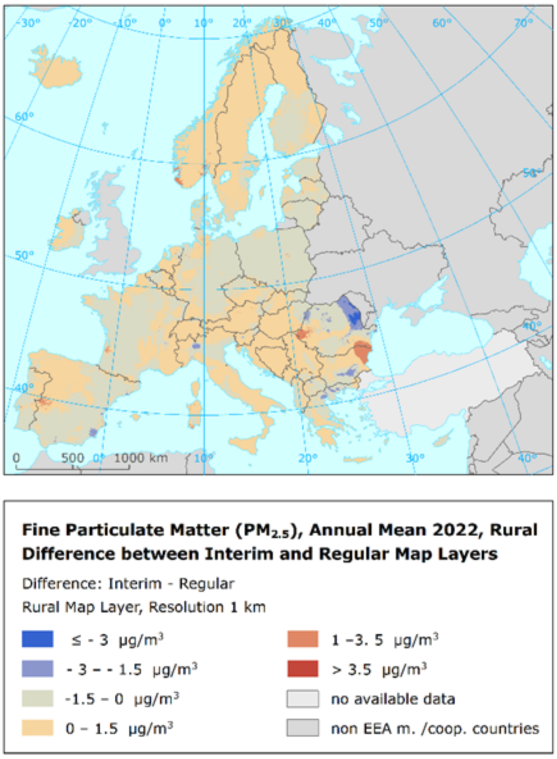

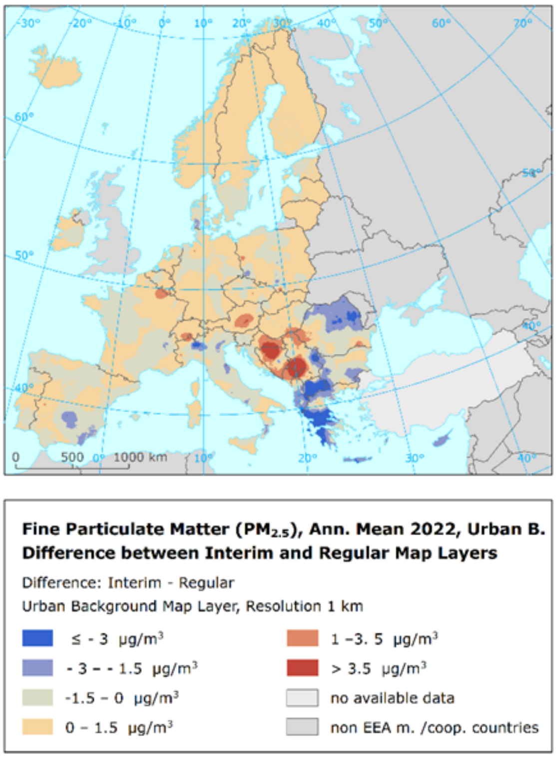

O_3

Table A4.5 shows the evaluation of the interim 2022 map for the O_3 indicator SOMO35, against the E1a data for 2022. The reason for the evaluation of the SOMO35 map is that in Horálek et al. (2023b), the interim map of this O_3 indicator was presented, not the peak season indicator. The evaluation is shown separately for two subsets of the stations (i.e. for stations with and without the E2a data). Again, the table also presents the cross-validation evaluation of the regular 2022 map for SOMO35 (Horálek et al., 2024b) based on the same subsets of the E1a station data, for comparable reasons.

Table A4.5: Validation of interim (left) and regular (right) map of the O_3 indicator SOMO35 for 2022 showing RMSE, RRMSE, bias, R^2 and linear regression from validation scatter plots in rural background (top) and urban background (bottom), against two validation sets of stations. Units: µg/m³·d except for RRMSE and R^2

Ozone – SOMO35											
Area	Validation set	Interim map					Regular map				
		RMSE	RRMSE	Bias	R^2	Regr. eq.	RMSE	RRMSE	Bias	R^2	Regr. eq.
Rural	E1a stations – all	1376	23.9%	86	0.655	y = 0.689x + 1872	1355	23.6%	20	0.663	y = 0.679x + 1866
	E1a stations with no E2a data	1883	31.0%	426	0.642	y = 0.694x + 2284	1801	29.7%	85	0.652	y = 0.668x + 2101
Urban backgr.	E1a stations – all	1502	30.5%	-22	0.553	y = 0.585x + 2023	1433	29.1%	7	0.591	y = 0.607x + 1943
	E1a stations with no E2a data	2725	50.8%	-367	0.204	y = 0.261x + 3285	2436	45.4%	-59	0.457	y = 0.494x + 2487

The results show that the uncertainty of the interim map is only slightly worse compared to the uncertainty of the regular map.

Additionally, the validation of the E2a data used in the interim O_3 mapping has been performed, see Table A4.6. In the case of O_3, the pseudo stations are not used in the interim mapping.

Table A4.6: Validation of E2a data showing RMSE, RRMSE, bias, R^2 and linear regression from validation scatter plots for rural background (top) and urban/suburban background stations (bottom), O_3 indicator SOMO35 for 2022. Validation by E1a station data. Units: µg/m³·d except for RRMSE and R^2

Ozone – SOMO35							
Station type	Evaluated set	Validation set	RMSE	RRMSE	Bias	R^2	Regr. eq.
Rural background	E2a stations	E1a stations with E2a data	283	4.8%	35	0.984	y = 1.019x - 74
Urban/suburban background	E2a stations	E1a stations with E2a data	215	4.3%	-37	0.989	y = 1.007x + 5

Map A4.3 shows the difference between the interim and the regular maps of the O3 indicator SOMO35 for 2022, for rural and urban background map layers. The major differences can be seen in in Balkan area, i.e. in the areas with the lack of the E1a stations.

Map A4.3: Difference between interim and regular map for O_3 indicator SOMO35 for 2022 in rural (left) and urban background (right) areas. Urban map layer is applicable in urban areas only

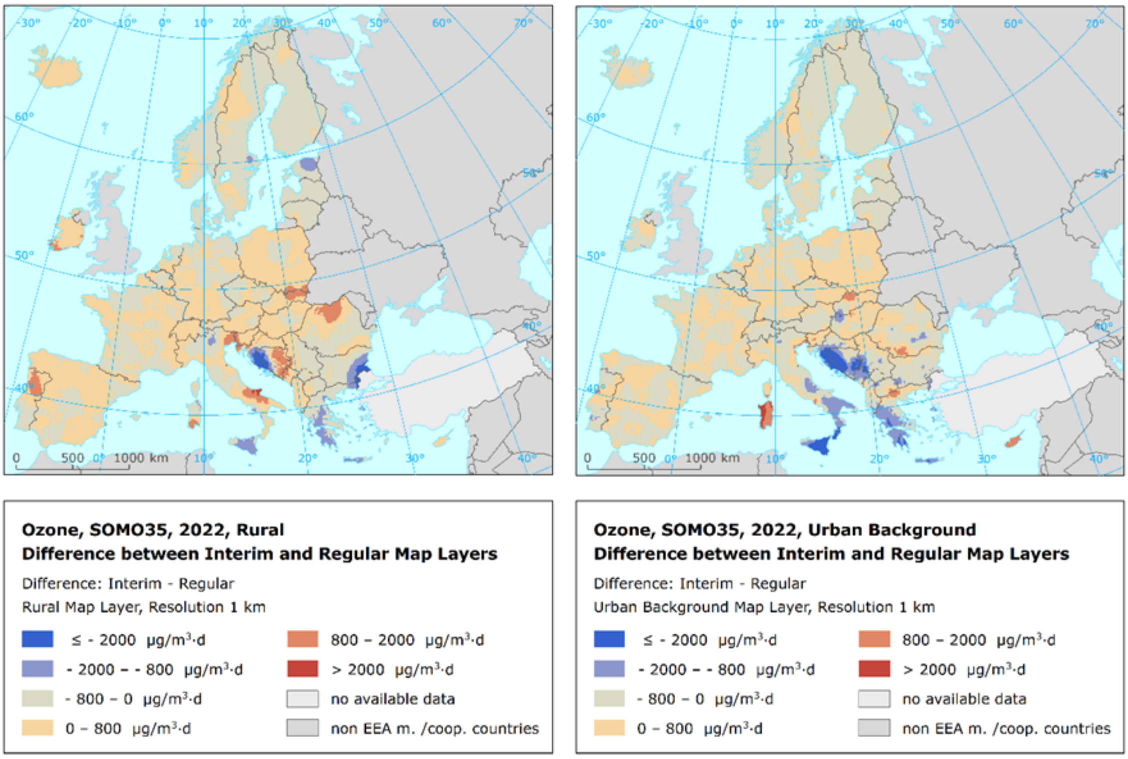

NO_2

Table A4.7 presents the evaluation of the interim NO_2 annual average 2022 map, against the E1a station data for 2022. Additionally, it also presents the cross-validation evaluation of the regular NO_2 annual average 2022 map (Horálek et al., 2024b) for the same subsets of the E1a station data, for comparable reasons.

Table A4.7: Validation of interim (left) and regular (right) map of NO_2 annual average 2022 showing RMSE, RRMSE, bias, R^2 and linear regression from validation scatter plots in rural background (top), urban background (middle) and urban traffic areas (bottom), against two validation sets of stations. Units: µg/m³ except for RRMSE and R^2

NO_2 – Annual Average											
Area	Validation set	Interim map					Regular map				
		RMSE	RRMSE	Bias	R^2	Regr. eq.	RMSE	RRMSE	Bias	R^2	Regr. eq.
Rural	E1a stations – all	2.1	33.3%	0.1	0.764	y = 0.809x + 1.3	2.2	35.3%	0.0	0.733	y = 0.756x + 1.5
	E1a stations with no E2a data	3.0	66.5%	-0.2	0.522	y = 0.655x + 1.4	2.9	65.5%	0.0	0.528	y = 0.644x + 1.6
Urban background	E1a stations – all	3.8	24.6%	-0.1	0.613	y = 0.627x + 5.6	3.9	25.7%	0.0	0.588	y = 0.657x + 5.2
	E1a stations with no E2a data	4.8	31.4%	-0.7	0.575	y = 0.581x + 5.8	4.8	31.2%	-0.1	0.575	y = 0.608x + 5.9
Urban traffic	E1a stations – all	5.7	23.2%	0.0	0.531	y = 0.542x + 11.4	5.8	23.6%	0.0	0.523	y = 0.584x + 10.3
	E1a stations with no E2a data	5.5	21.9%	0.2	0.526	y = 0.528x + 12.1	5.2	20.6%	0.0	0.582	y = 0.596x + 10.2

One can see that the uncertainty of the interim map is at the same level as the uncertainty of the regular map.

Additionally, the validation of the E2a data and the pseudo station data used in the interim NO_2 mapping has been performed. Table A4.8 shows the validation of the E2a and the pseudo data, against the E1a station data in the locations of these stations.

Table A4.8: Validation of E2a and pseudo station data showing RMSE, RRMSE, bias, R^2 and linear regression from validation scatter plots for rural background (top), urban/suburban background (middle) and urban/suburban traffic stations (bottom), NO_2 annual average 2022. Validation by E1a station data. Units: µg/m³ except for RRMSE and R^2

NO_2 – Annual Average							
Station type	Evaluated set	Validation set	RMSE	RRMSE	Bias	R^2	Regr. eq.
Rural background	E2a stations	E1a stations with E2a data	0.2	3.2%	0.0	0.998	y = 0.997x
	Pseudo stations	E1a stations in locations of pseudo stations	1.6	30.2%	0.2	0.872	y = 0.852x + 0.5
Urban/suburban background	E2a stations	E1a stations with E2a data	0.3	2.1%	0.0	0.997	y = x
	Pseudo stations	E1a stations in locations of pseudo stations	2.6	16.8%	0.5	0.879	y = 0.922x + 0.7
Urban/suburban traffic	E2a stations	E1a stations with E2a data	0.6	2.3%	0.0	0.996	y = x
	Pseudo stations	E1a stations in locations of pseudo stations	2.0	7.5%	0.0	0.928	y = 0.925x + 2.0

The results show worse agreement of the pseudo data with the E1a data in the rural areas, quite similar agreement in the urban background areas and better agreement in the urban traffic areas, compared to the validation of the pseudo stations presented in Horálek et al. (2021a), which recommended the use of the pseudo stations.

Map A4.4 shows the difference between the interim and the regular maps of NO_2 annual average 2022, for rural and urban background map layers. The main differences can be seen in the urban areas of the west Balkan (especially Bosnia) and Romania. In the first case, the reason probably is in the lack of the E2a data for Bosnia (where the E1a data show high NO_2 values). In the second case, the reason lies in a lack of several stations with the E2a data (with high NO_2 values) in the E1a data set.

Map A4.4: Difference between interim and regular map for NO_2 annual average 2022 in rural (left) and urban background (right) areas. Urban map layer is applicable in urban areas only

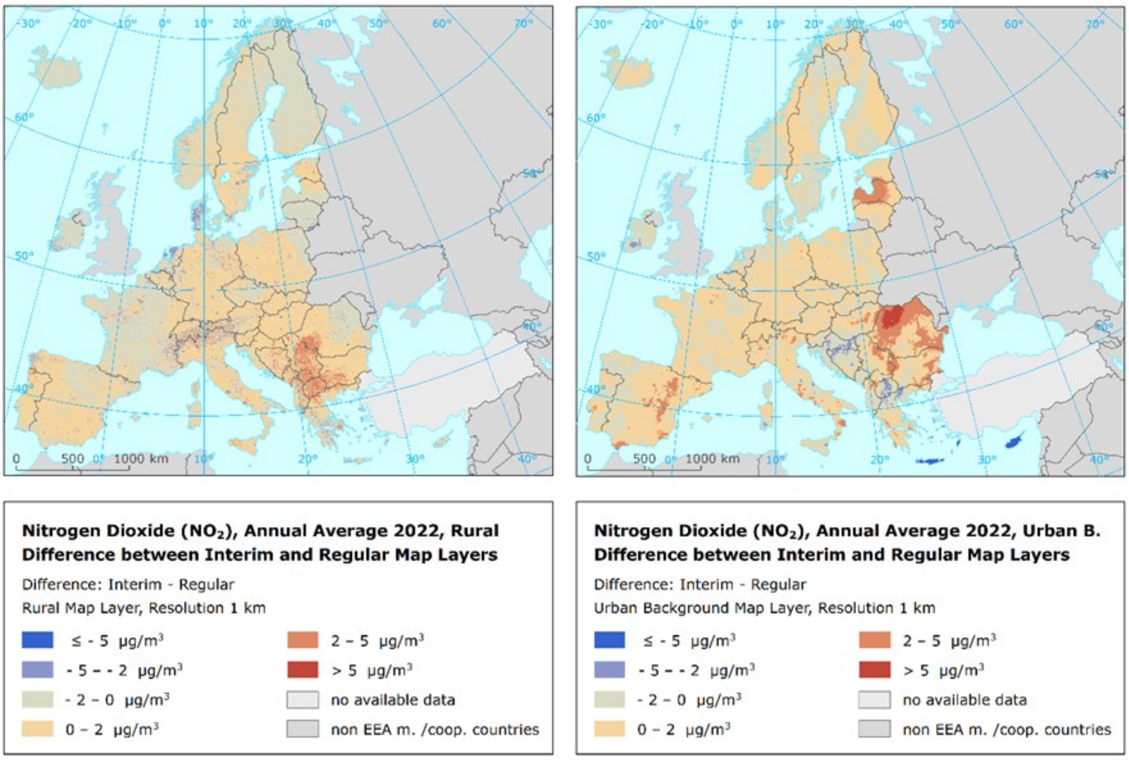

A4.2 Population exposure

This section shows the exposure tables based on the interim maps for 2022 (constructed using the non-validated E2a measurement data) as presented in Horálek et al. (2023b) and compares them with the exposure tables based on the 2022 regular maps (Horálek et al., 2024b), which were constructed using the validated E1a measurement data. In agreement with the conclusions of Horálek et al. (2023a), only the exposure estimates for the EU-27, the large regions and the total considered area are presented in the exposure tables based on the interim maps.

Table A4.9 shows the population-weighted concentration of PM_{10} annual average and the percentage of population living in areas with concentrations above the PM_{10} annual Limit Value (LV) of 40 µg/m^3, as well as the population-weighted concentration of $PM_{2.5}$ annual average and the percentage of population living in areas with concentrations above the PM_{10} annual LV of 25 µg/m^3, for 2022. The results are presented for the large regions, for the EU-27 and for the total mapping area, based on both the interim and the regular maps. Next to the values calculated based on the interim and regular maps, the table presents also the differences between the values calculated based on these two maps.

Table A4.9: Population-weighted concentration and percentage of population living in areas in exceedance of annual LV for PM_{10} annual average (left) and $PM_{2.5}$ annual average (right) for 2022 based on the interim and regular maps and the difference "Interim – Regular"

Region	PM_{10} Annual Average 2022						Region	$PM_{2.5}$ Annual Average 2022					
	Population-weighted concentration [µg/m³]			Population above LV of 40 µg/m³ [%]				Population-weighted concentration [µg/m³]			Population above LV of 25 µg/m³ [%]		
	Interim	Regular	Diff.	Inter.	Reg.	Diff.		Interim	Regular	Diff.	Inter.	Reg.	Diff.
Northern Europe	11.5	11.3	**0.1**	0.0	0.0	0.0	Northern Europe	6.2	6.1	**0.1**	0.0	0.0	0.0
Western Europe	16.5	16.6	**-0.1**	0.0	0.0	0.0	Western Europe	9.5	9.4	**0.1**	0.0	0.0	0.0
Central Europe	17.5	17.4	**0.1**	0.0	0.0	0.0	Central Europe	11.6	11.6	**0.1**	0.0	0.3	-0.3
Southern Europe	22.2	22.7	**-0.5**	0.0	0.5	-0.5	Southern Europe	12.1	12.8	**-0.6**	0.0	0.1	-0.1
South-eastern Europe	24.3	23.9	**0.4**	3.0	2.0	1.0	South-eastern Europe	15.9	16.3	**-0.4**	6.3	5.6	0.8
Total	**19.1**	**19.1**	**0.0**	**0.3**	**0.4**	**0.0**	**Total**	**11.5**	**11.7**	**-0.2**	**0.7**	**0.7**	**0.0**
EU-27	**18.8**	**19.0**	**-0.1**	**0.0**	**0.2**	**-0.2**	**EU-27**	**11.3**	**11.5**	**-0.2**	**0.0**	**0.2**	**-0.2**

One can see that for the total mapping area and for the EU-27, the population-weighted concentration show almost the same results in both variants, for both PM_{10} and $PM_{2.5}$. The same is true also for the Northern, Western and Central Europe, while the Southern and South-eastern Europe show slight differences. Similar numbers are given also for the population exposed to concentrations above LV, with slight difference also in the Central Europe, in the case of $PM_{2.5}$.

Table A4.10 shows the population-weighted concentration of the O_3 indicator SOMO35 and the percentage of population exposed to the SOMO35 values above 6000 µg/m³·d, and also the population-weighted concentration of NO_2 annual average and the percentage of population living in areas with concentrations above the NO_2 annual LV of 40 µg/m³, for 2022. The results are presented in the same structure as Table A4.9.

Table A4.10: Population-weighted concentration and percentage of population living in areas in exceedance of annual LV for O_3 indicator SOMO35 (left) and NO_2 annual average (right) for 2022 based on the interim and regular maps and the difference "Interim – Regular"

Region	O_3, SOMO35, 2022						Region	NO_2 Annual Average 2022					
	Population-weighted concentration [µg/m³·d]			Population above LV 6000 µg/m³·d [%]				Population-weighted concentration [µg/m³]			Population above LV of 40 µg/m³ [%]		
	Interim	Regular	Diff.	Inter.	Reg.	Diff.		Interim	Regular	Diff.	Inter.	Reg.	Diff.
Northern Europe	2 067	2 199	**-133**	0.0	0.0	**0.0**	Northern Europe	7.3	7.7	**-0.4**	0.0	0.0	**0.0**
Western Europe	4 098	4 099	**-1**	2.6	2.3	**0.3**	Western Europe	13.5	13.8	**-0.3**	0.5	0.4	**0.1**
Central Europe	4 811	4 758	**53**	10.2	8.4	**1.8**	Central Europe	13.7	13.8	**-0.1**	0.0	0.0	**0.0**
Southern Europe	5 905	6 033	**-129**	39.6	43.4	**-3.8**	Southern Europe	15.6	16.3	**-0.7**	0.3	0.5	**-0.2**
South-eastern Europe	4 126	4 286	**-159**	7.3	9.8	**-2.4**	South-eastern Europe	15.9	15.6	**0.3**	0.1	0.1	**0.0**
Total	**4 755**	**4 799**	**-44**	**16.7**	**17.4**	**-0.6**	**Total**	**14.0**	**14.3**	**-0.3**	**0.2**	**0.2**	**0.0**
EU-27	**4 755**	**4 793**	**-38**	**16.5**	**17.0**	**-0.5**	**EU-27**	**14.1**	**14.4**	**-0.3**	**0.2**	**0.2**	**-0.1**

For the O_3 indicator SOMO35, the table shows again a good agreement of the results based on the interim and regular maps for the total area and for the EU-27, as well as for the Northern, Western and Central Europe. For the Southern and South-eastern Europe, the results based on the interim map are slightly lower, compared to the results based on the regular map. For the NO_2 annual average, the population-weighted concentration based on the interim map gives slightly lower numbers for the total area and the EU-27, compared to the results based on the regular map. For the population exposed to concentrations above the NO_2 annual LV of 40 µg/m^3, the results based on the interim and the regular maps are almost the same.

In general, one can conclude that the population exposure estimates based on the interim maps give a good agreement for the total area, the EU-27 and the regions of the Northern, Western and Central Europe, while slightly larger differences for the regions of the Southern and South-eastern Europe, where the E2a data show larger gaps for some countries.

European Topic Centre on
Human Health and the Environment
https://www.eionet.europa.eu/etcs/etc-he

The European Topic Centre on Human Health and the Environment (ETC HE) is a consortium of European institutes under contract of the European Environment Agency.

European Environment Agency
European Topic Centre
Human health and the environment